Saline surface water across the southern Norfolk and Suffolk Broads during August 2026: field observations and drought-conditioned comparisons

Michael Natusch*
Independent researcher

13 November 2026
Non-peer-reviewed preprint submitted to EarthArXiv

Abstract

Saltwater entering tidal rivers can affect freshwater habitats and water use, but high salinity during drought is not necessarily historically unusual. This regional case study compares 36 surface-water observations from the southern Norfolk and Suffolk Broads on 16 to 20 August 2026 with historical chemistry and flow- and tide-conditioned models. Salinity varied substantially between places and times. Nine observations were polyhaline or euhaline equivalents, indicating strongly brackish to seawater-like water. On 19 August, observations of mesohaline-or-higher water spanned approximately 19 km between sampled endpoints on the Yare and Waveney; this was not a continuously mapped or simultaneous plume. A direct Oulton Broad reading exceeded the retrieved local conductivity maximum by 18.4%, although the drought archive was too sparse to establish its rarity under comparable conditions. At Chet Mouth and Reedham, selected dilution-derived readings exceeded a specified family of summer flow- and tide-conditioned comparisons. These are exploratory model departures: severe-drought validation is sparse, systematic measurement uncertainty remains and broader error scenarios include the observations. Some lower-estuary readings were compatible with historical drought expectations. The contribution is a documented pattern of surface exposure across connected reaches, with explicit distinctions between local archive exceedance and exploratory model departures. The probability of an exceptional event across the surveyed network remains unvalidated. Repeated exposure could constrain freshwater habitats and water use under future low-flow and sea-level changes. Ecological damage and climate attribution were not established.

Keywords: salinity intrusion; drought; estuaries; Norfolk Broads; tidal forcing; surface water.

1 Introduction

Freshwater inflow and seawater exchange jointly determine the salinity of an estuary. Low river flow reduces freshwater dilution, while tides, coastal water levels and mixing control the transport and storage of salt. A saline incursion can consequently affect several connected reaches and remain visible after the incoming tide has turned. Its significance concerns both the concentration at individual sites and the geographical extent and duration of exposure [15].

The Norfolk and Suffolk Broads provide an important setting for this interaction. Their connected rivers, shallow waters and managed low-lying landscape support freshwater and estuarine habitats alongside navigation, farming and fisheries. A survey of the Yare, Waveney, Chet and connected waters between 16 and 20 August 2026 encountered a wide range of surface-water conductivities, including water with a seawater-equivalent salinity above 18 well inland. The survey took place during a declared regional drought [10, 13].

*Correspondence: m.natusch@physics.org. ORCID: https://orcid.org/0000-0002-9813-4503

There are two complementary questions. First, how extensive and persistent was the observed saline-water pattern? Second, which observations were higher than expected for their own location, flow, tide, season and preceding conditions? High salinity can be ecologically relevant even where it is consistent with historical drought behaviour. Conversely, an unusually high percentile in a freshwater reach need not represent a large absolute salt concentration. The spatial synthesis and the location-specific comparisons therefore answer different parts of the same environmental question.

We address three statistical questions: (1) what historical non-drought conditions look like at the visited locations, (2) what typical historical drought conditions look like there and (3) whether the field observations exceed those expectations after conditioning on available forcing. We also describe salinity classes, repeated visits and river-network spans. These descriptive results establish the scale of the observed pattern without treating unsampled water or unobserved hours as measurements.

The Broadland Futures Initiative (BFI) commissioned statistical models of saline intrusions from HR Wallingford [18]. That report provides relevant process variables, fixed-gauge models and continuous-monitoring context. We use its published coefficients as a benchmark, while developing a separate historical comparison for the field observations. Neither fixed-gauge equations nor a more complex machine-learning model automatically provide validated predictions at arbitrary boat coordinates.

Recent fieldwork and models show why connected-channel behaviour matters. A 17-week drought campaign in the Rhine-Meuse Delta combined fixed sensors and ship transects and identified different controls in main and side channels [36]. A process model of that network also found channel-dependent salt transport and adjustment times [5]. Those studies provide methodological context, not transferable response coefficients for the Broads. In the Pamlico River Estuary, coupled catchment and estuary modelling further shows how discharge seasonality, sea-level rise and local bathymetry interact to shape salt-front movement [37]. Such process studies caution against interpreting distance inland through river flow alone.

Data-driven approaches also provide useful comparisons. Zhu and colleagues coupled catchment rainfall-runoff models with machine learning to predict daily salinity at ten Scheldt stations [38]. Cong and colleagues evaluated multi-day salinity forecasts at one Mekong Delta station using a complete dry season excluded from development [9]. These studies illustrate the value of hydrological history and independent temporal evaluation. Their daily responses and monitoring populations differ from the instantaneous, geographically dispersed observations considered here.

The contribution of this study is the documented August 2026 southern Broads surface-water record and its explicit comparison with local archives, historical drought states and specified forcing-conditioned model families. The drought-salinity mechanism is well established. The particular question here is which local observations remain unusual under the available comparisons, and what can be said about their combined spatial pattern without assuming unmeasured continuity or a calibrated network-wide event probability.

This is an exploratory observational study. The field observations motivated the hypothesis and the choice of detailed follow-up locations. Field salinity was excluded from historical coefficient fitting and residual calibration, but the analysis is not a preregistered hypothesis test. Evidence of a broad saline-water episode is assessed jointly with the strength and limits of individual comparisons, rather than by counting correlated observations as independent statistical confirmations.

2 Study setting and observations

2.1 Field survey

The dataset comprises 36 conductivity observations at 27 exact coordinate pairs, grouped into 24 nearby location identities, collected on 16 to 20 August 2026. The locations include the lower

Yare and Waveney, Reedham and the Chet confluence, the Chet towards Loddon, Herringfleet, Beccles, Oulton Broad and Oulton Dyke, as well as upper-Yare and side-water locations. All river samples were collected from the surface close to the river centre. This describes the sampled layer; it is not a whole-water-column average. One submitted coordinate is retained without a reliable waterbody assignment.

There are 21 undiluted readings and 15 precisely prepared dilutions. Conductivity was measured with an Apera EC20 meter, whose stated range reaches 20 mS cm^{-1} and whose specified accuracy is ±1% of full scale plus one display digit [1]. For samples requiring dilution, one volume of river water was mixed with two or three volumes of tap water. The investigator confirmed that the stated volumes were measured precisely. The associated tap-water conductivity is retained for each diluted sample. No arbitrary dilution-volume error is imposed and no observation is excluded because its value is high.

Date, British Summer Time (BST, UTC+1), coordinates, conductivity display, temperature, dilution ratio and tap control form the field record in Appendix A. Temperatures are those displayed during measurement and may differ from river temperature at collection where water was measured in a vessel. The reference temperature of the instrument's conductivity compensation was not independently recorded. Conductivity referenced to 25 °C is the working scale, with a 20 °C reference sensitivity retained.

This was an opportunistic moving survey with some repeated locations, not a random or simultaneous survey of the network. Differences between successive locations combine spatial and temporal change. At Chet Mouth, Herringfleet, Beccles and Oulton Dyke, repeated coordinates allow direct description of within-location variation. The investigator reported prolonged rain during the night of 19 to 20 August. This is contextual information rather than a reconstructed catchment rainfall input or an attribution of subsequent freshening.

2.2 Historical chemistry and hydrological context

Historical chemistry comes from the Environment Agency (EA) Water Quality Archive [12]. Conductivity referenced to 20 °C, conductivity referenced to 25 °C, in-situ salinity and chloride-derived salinity retain separate method labels. Sample material, result qualifiers, source quality flags and station identity are preserved. Exact numeric observations before 1 January 2026 provide the historical reference. Multiple same-station, same-date observations are represented by a median where station-day distributions are used.

The five substantial direct-salinity stations are Burgh Castle, Berney Arms Mill, the Breydon Water main channel, north of Cobham Island and Haven Bridge. Their descriptive distributions contain 827 eligible pre-2026 station-days, of which 212 fall in July to September and 65 in August. They supply estuarine context, not a substitute for inland baselines. Four suspect zero values from one July 2021 sampling run are retained in the audit but excluded from the primary histograms. Method and inclusion details are in Appendix C.

Oulton Broad Yacht Station supplies a local conductivity archive even though it lacks a substantial direct-salinity series. Its primary native-EC25 lake-water cohort comprises 46 station-days in five sampled years: 2000, 2001, 2002, 2019 and 2020. A separate EC20 series and chloride measurements provide method checks. St Olaves supplies historical reach context for Herringfleet. Other inland comparisons use river-specific native-conductivity cohorts or explicitly qualified proxies. Winter and spring logger deployments near Church Farm and Loddon are kept separate from summer drought baselines.

River flows were obtained through the EA Hydrology and National River Flow Archive services [11, 33]. The Yare inflow index sums the Yare at Colney, Tas at Shotesham and Wensum at Costessey. These gauges cover distinct tributary catchments totalling 949.2 km^2. A broader regional index additionally includes the Waveney at Needham and Bure at Horstead, totalling 1,632.2 km^2. These are sums of observed gauged flows, not estimates obtained by scaling discharge to every ungauged catchment area. They do not measure local tidal transport, Chet discharge or

Oulton flushing. Gauge areas, topology and flow-state comparisons are given in Appendix D.

Historical and provisional 2026 sea levels provide astronomical and observed coastal forcing [6, 16, 35]. Coastal features use level anomalies and recent tidal ranges rather than transferring absolute vertical datums between unrelated gauges. Local level observations support timing checks. The flow and tidal histories contain reconstruction scenarios where observations are missing; those scenarios remain distinguishable from measured inputs.

3 Methods

3.1 Conductivity, seawater equivalents and descriptive classes

Let $F_T(C)$ be practical salinity calculated from conductivity C at reference temperature T and zero sea pressure, using the Gibbs SeaWater implementation of PSS-78 with its low-salinity extension [22, 34]. Let G_{25} be the reverse conversion at 25 °C. We call the result *seawater-equivalent practical salinity*, S_{eq}, because river and tap-water ionic composition need not match diluted seawater. Practical salinity is dimensionless and is not a direct salt-mass measurement.

For one volume of river water and r volumes of tap water, the working reconstruction is

$$S_{\mathrm{eq}} = (1 + r)F_{25}(C_m) - rF_{25}(C_t), \tag{1}$$

$$C_{25,\mathrm{eq}} = G_{25}(S_{\mathrm{eq}}), \tag{2}$$

where C_m and C_t are the measured mixture and tap conductivities. For undiluted water, $r = 0$ and the conductivity round-trip reproduces the display. This accounts for the nonlinearity of conductivity with seawater salinity, but volume-weighting a seawater equivalent is not exact salt-mass conservation for arbitrary ionic mixtures and densities. Natural-water conductivity depends on composition as well as concentration [27]. Appendix B specifies the assumptions and sensitivities.

We apply conventional descriptive salinity bands to S_{eq}: fresh below 0.5, oligohaline from 0.5 to below 5, mesohaline from 5 to below 18, polyhaline from 18 to below 30, euhaline from 30 to below 40 and hyperhaline at 40 or above [14]. They provide an accessible description of the observations. They are neither biological damage thresholds nor tests of historical unusualness. In particular, dissolved freshwater ions can materially influence the oligohaline-equivalent range. Class boundaries are applied consistently as lower-inclusive and upper-exclusive intervals.

For the historical comparison, calibration records and independent reference-solution checks for the field campaign are not available in the supplied record. The following allowances must therefore not be read as a complete measurement-uncertainty budget. Instrument allowances are $0.21\,\mathrm{mS\,cm^{-1}}$ in the $20\,\mathrm{mS\,cm^{-1}}$ display range and $0.021\,\mathrm{mS\,cm^{-1}}$ in the $2{,}000\,\mu\mathrm{S\,cm^{-1}}$ range. Opposing mixture and tap endpoints are propagated through Equation 1. These are specification-based limits, not confidence intervals, and exclude unquantified calibration, composition and reference-setting effects. Class assignments are checked against both endpoints. Native historical EC20 enters only explicit conversion scenarios, including a separate ±10% bridge sensitivity, rather than being silently pooled with native EC25.

3.2 Historical expectations and drought definition

Three distributions answer the study questions. $F_{s,N}$ describes historical non-drought conditions at location s, $F_{s,D}$ describes historical drought conditions and $F_{s,t}$ conditions on the available forcing at a particular visit. P90 and P95 denote the 90th and 95th percentiles of the stated distribution. An archive percentile describes sampled dates, not the fraction of elapsed time spent below that value.

Drought requires a seven-day mean flow, Q_7, below the seasonal P20 for at least 14 consecutive valid days. Seasonal thresholds use 1991 to 2020 and a ±15-day day-of-year window. Short

low-flow runs and the subsequent 28-day recovery period remain separate. "Normal" means July to September non-drought dates under this rule. It is not synonymous with absence of every type of water stress. The rule is applied to the relevant gauged index; a regional drought declaration does not force every tributary into the same class.

Historical calendar distributions combine hourly forcing states with withheld-year residual distributions. If $\widehat{\eta}_{s,h}$ is the fitted prediction on the model scale at historical hour h and e_j is a calibration residual,

$$\widehat{F}_{s,r}(c) = \sum_{h,j} w_{h,r} v_j \, \mathbf{1}\left[g_+^{-1}(\widehat{\eta}_{s,h} + e_j) \le c\right], \qquad r \in \{N, D\}. \tag{3}$$

Weights sum to one within each population. Percentiles come from the complete mixture; separate percentiles of central predictions and residuals are not added. Flow and coast retain their historical pairing. Equal-episode weighting tests whether long drought episodes dominate the results. Ranges across model variants express sensitivity, not confidence intervals for a single percentile.

3.3 Models, tidal forcing and antecedent conditions

The principal lower-Yare model is a regularised regression with river distance, annual season, flow history, M2 tidal phase and optional observed coastal predictors:

$$g(C) = \beta_0 + f_x(x) + f_a(d) + f_Q(x, Q_7, Q_{28}) + f_M(x, t) + f_H(x, H_{72}, R_{25}) + \epsilon. \tag{4}$$

The response is either numerical conductivity or $\log(1 + C/C_0)$, with $C_0 = 1\,\mathrm{mS\,cm^{-1}}$. The fixed basis uses quadratic or radial spatial terms, harmonic terms and specified interactions. Ridge penalisation is 10 after standardisation. Station and within-station year weights prevent the most frequently sampled station from determining the fit. Two historical clock interpretations and separate conductivity-method tracks represent uncertainties in older records.

H_{72} is a preceding 72-hour coastal level anomaly and R_{25} a preceding 25-hour level range. Both complement the M2 harmonic. High water is not assumed to coincide with maximum salinity or zero velocity. Historical coastal gaps are reconstructed and evaluated through withheld-block errors. Daily flow source windows are joined with the established two-day reporting offset. A missing hour of Tas observations receives independently tested reconstruction scenarios as well as a deliberately broader unreconstructed alternative. Details and validation are in Appendices D and E.

The dynamic family smooths selected forcing drivers on a 15-minute grid:

$$z_t = e^{-\Delta t/\tau} z_{t-1} + (1 - e^{-\Delta t/\tau}) u_t, \tag{5}$$

using response times of 0, 24, 72 and 168 hours. For $\tau = 0$, $z_t = u_t$; the exponential expression applies for $\tau > 0$. Annual and M2 harmonics remain unfiltered. Initial-state and residual missing-forcing weights are tracked. August salinity does not enter as a recursive state. This is a distributed-lag regression, not a hydrodynamic salt-balance model.

Upper-Yare native-conductivity models and lower-estuary direct-salinity station models remain distinct. For the latter, field S_{eq} is compared with the EA model's reported-ppt scale as an explicitly approximate cross-method comparison. A depth scenario of 0.1 m represents a surface-oriented model scenario, not a measured collection depth. No Yare model is extended into the Waveney or Oulton without validation. The BFI occurrence/intensity model and alternatives such as deterministic transport and decomposition/random-forest prediction are considered separately in Appendix F.

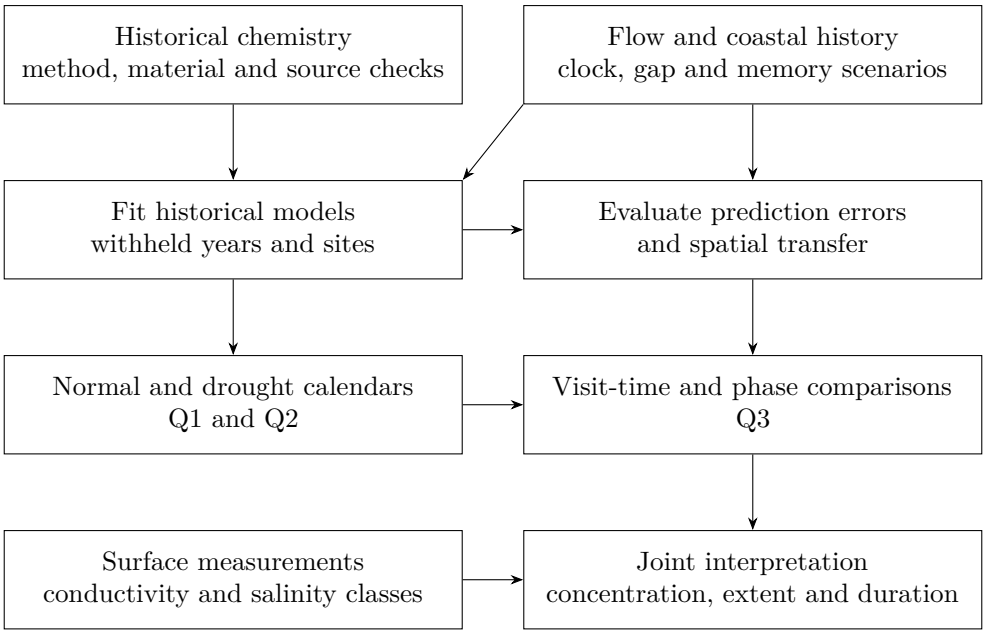


Figure 1: Analysis structure. Field responses enter comparison and synthesis but do not enter historical coefficient fitting or residual calibration. The arrows denote analytical use, not causal identification. OpenAI ChatGPT/Codex assisted with the TikZ source code; exact historical model versions were not retained. The author reviewed the diagram.

3.4 Validation and sensitivity limits

Whole-year holdouts and target-station plus test-year holdouts address temporal and spatial dependence [28]. A local route transfers withheld-year residuals from a nearby station; a stricter unknown-site route also excludes the target station from calibration. They answer different validation questions. Fixed-gauge errors are not assumed to be identical at a boat coordinate merely because the distance is short.

A nominal conditional upper comparison is

$$U_{.95}(s,t) = g_{+}^{-1}\{\widehat{\eta}(s,t) + q_{.95}(e)\}\,. \tag{6}$$

It is not guaranteed to achieve 95% coverage. Phase sensitivity replaces the fitted M2 sine/cosine contribution by its maximum amplitude while retaining the other forcings. Omitted-year tests regenerate both fits and residual calibration. Coastal-error scenarios preserve errors shared by observations affected by the same gap. The joint experiment combines the two most adverse year deletions per model with 100 coastal-error draws and a central case; it is not an exhaustive set of joint errors.

An observation exceeds a stated sensitivity family if its instrument-only lower endpoint exceeds that family's largest upper comparison. The primary summer family retains internally checked flow reconstruction, phase, method, clock, response-memory and historical-error sensitivities. The missing-flow alternative and the largest historical residual from any season are reported separately. An exceedance of this family is an exploratory model departure, not a calibrated test with a known false-positive rate. These maxima are neither simultaneous confidence bounds nor universal physical limits. Some combinations are deliberate algebraic stress tests rather than jointly observed physical states.

3.5 Spatial and episode-scale synthesis

We retain exact sample times and distinguish survey-network span from the span between selected salinity-class observations. River distance follows the mapped channel network and counts shared

segments once within each reported route definition. It does not measure a continuous front, the boat's actual travelled distance or the length proven anomalous at every point. Network calculations and routing assumptions are supplied in Appendix G.

The spatial pattern is assessed through concentration, its distribution across connected reaches and repeated visits. No binomial test treats the fraction of high observations as a random sample of the Broads. Shared tides, water masses, instrument calibration and reconstruction assumptions create dependence. A broader event interpretation is therefore descriptive and mechanistic, while claims of departure from historical expectations retain the site-specific validation limits.

3.6 Computational implementation and AI assistance

OpenAI ChatGPT/Codex assisted with research programming, model implementation, checking and figure code. The reported calculations were executed in Python rather than inferred from language-model responses. The archived reconstruction used Python 3.12.14, NumPy 2.3.5, pandas 2.2.3, SciPy 1.17.0, Matplotlib 3.10.8, openpyxl 3.1.5 and GSW 3.6.23. Package-relative scripts, input hashes, figure lineage and numerical comparison logs are supplied. Exact identifiers of the AI models used in every historical session are unavailable and no version is inferred from the product name.

The 12 data figures are reproducible plots of the supplied observations or numerical outputs, rendered using programmatically specified coordinates, axes and labels. No generative image model created or altered these data figures. The explanatory workflow diagram is rendered from TikZ code. Author review and approval cover the final science, references, data and code; internal numerical agreement is distinguished from independent empirical validation.

4 Results

4.1 A broad but heterogeneous saline-water pattern

Working conductivity spans 1.086 to 55.440 $\mathrm{mS\,cm^{-1}}$, corresponding to S_{eq} of approximately 0.54 to 36.77. The upper end is reconstructed from dilution, not a direct meter reading of the source water. The 36 observations comprise 14 oligohaline, 13 mesohaline, five polyhaline and four euhaline equivalents. None changes class within the retained instrument-only endpoints. Four change under the separate 20 °C reference scenario, illustrating the distinction between instrument precision and systematic assumptions.

Figure 2 shows a spatially extensive pattern across the connected survey area. On 19 August, 15 observations at or above $S_{\mathrm{eq}} = 5$ occur within a Yare endpoint span of 8.979 km and a Waveney endpoint span of 9.826 km. Their sum is **18.805 km**, with shared segments counted once within each named channel. Polyhaline-or-higher observations span 10.438 km across those channels. Both threshold-span results are unchanged when classification uses instrument lower endpoints.

The 18.8 km figure is the sum of along-channel distances between the outermost qualifying observations on each river. It is neither a simultaneous saline-front length nor the distance at which every point has been shown to exceed historical drought expectations. Including the qualifying Chet observations across the full survey period extends the corresponding mesohaline-or-higher spans to 21.757 km. These definitions are deliberately distinct from the broader mapped survey span of 55.284 km, which includes low-conductivity inland observations and excludes ambiguous off-centreline/open-water projections from its length calculation.

The Broads Authority describes more than 200 km of navigable rivers and broads [7]. The 18.8 km same-day endpoint spans are therefore of the order of one tenth of that published network length. This is a geographical scale comparison, not an estimate that one tenth of the Broads was anomalously saline. The substantive result is that high salinity was observed across substantial sections of two connected rivers, rather than only at one isolated site.

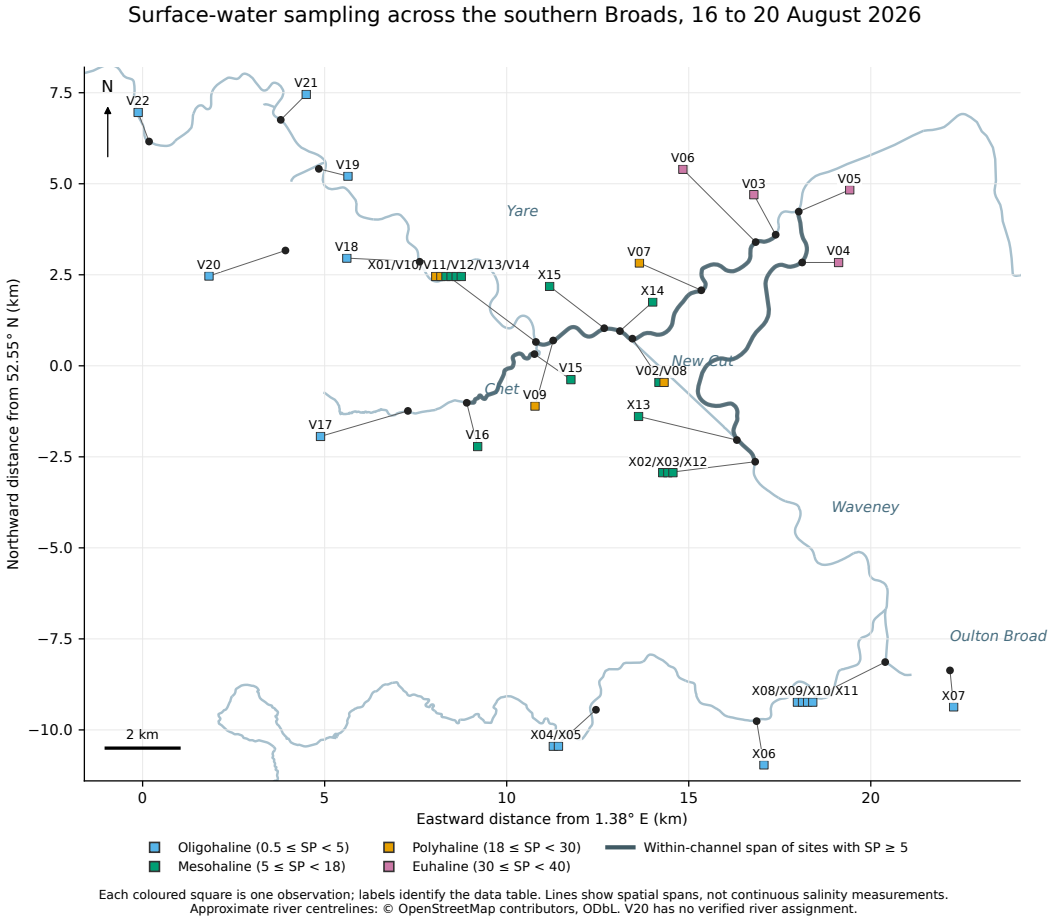


Figure 2: Surface-water observations and mapped waterways. Colours describe working seawater-equivalent salinity classes. Repeated coordinates represent separate times. The map does not interpolate a continuous salinity surface or assign the highest class to intervening unsampled water. Map data: © OpenStreetMap contributors, ODbL: `https://www.openstreetmap.org/copyright`. Bold channel segments show the full-period spans between mesohaline-or-higher observations, not only the 19 August subset. All quantified observations are retained, including the coordinate without a reliable waterbody assignment.

4.2 Salinity intensity and spatial ordering

Four lower-Yare and lower-Waveney observations on 19 August are euhaline equivalents, with S_{eq} from 30.79 to 36.77. Farther inland, Seven Mile Reach, New Cut, Reedham Ferry Reach and Chet Mouth include polyhaline equivalents from approximately 20.07 to 29.29. The sequence from 14:33 to 18:40 therefore places water with substantial marine-equivalent salt content across several inland Yare locations as well as the lower estuary (Figure 3). The observations are sequential, so location and tidal evolution remain confounded.

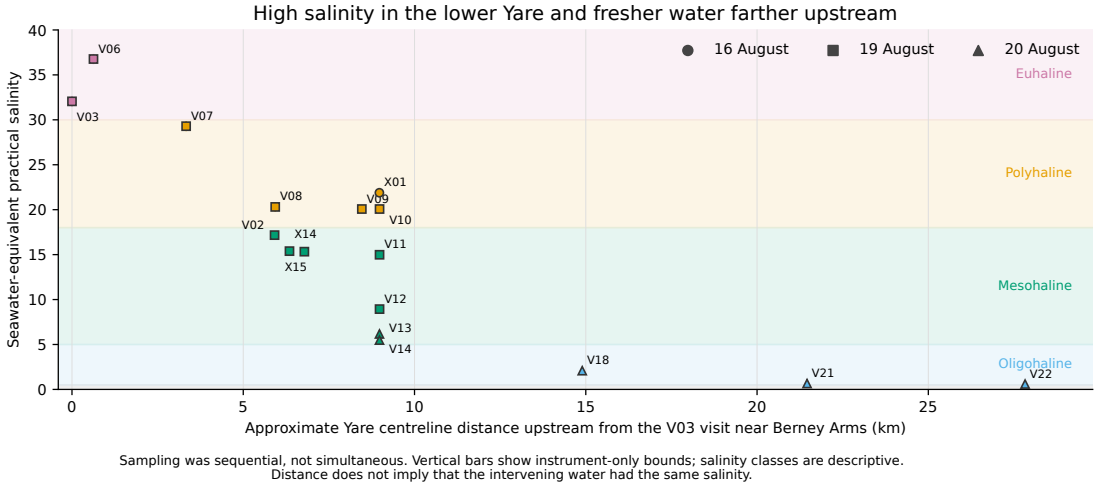


Figure 3: Along-river distribution of Yare observations, with times retained. River distance describes position, not a simultaneous transect. Changes between visits can reflect both spatial gradients and tidal evolution. The salinity scale is a working seawater equivalent.

The other waterways show both extension and attenuation of the pattern. Herringfleet has mesohaline equivalents of 10.92, 9.75 and 8.84 at the three visits on 16, 17 and 19 August. Oulton Broad and Oulton Dyke have oligohaline equivalents around 4.2 to 4.5. The Chet observations are mesohaline at the two lower sampled locations and oligohaline near Loddon. Beccles and several upper-Yare or side-water observations have much lower conductivity. Because freshwater ions can dominate near the low end, classifying those values as oligohaline equivalents does not establish marine intrusion everywhere in the survey.

4.3 Repeated sites reveal substantial temporal variation

Chet Mouth was polyhaline at 13:15 on 16 August ($S_{eq} = 21.89$) and at 18:40 on 19 August ($S_{eq} = 20.07$). On 19 August it subsequently fell to 14.98 at 20:40 and 8.94 at 22:50, both mesohaline. By 12:06 on 20 August it was 5.49 (Figure 4). From 19 August 18:40, the decrease was 55.5% in four hours ten minutes and 72.7% by the following midday. This is strong within-location change rather than an artefact of comparing different reaches.

At Oulton Dyke, four direct conductivities of 8.130, 7.600, 7.630 and 7.630 $\mathrm{mS\,cm^{-1}}$ span 18 hours 17 minutes, from 18 August 16:38 to 19 August 10:55. This establishes repeated brackish surface water at one coordinate, while leaving the intervening conditions unknown. Repeated visits reduce reliance on a single grab but do not make the observations independent. Similarly, the two high Chet Mouth dates do not demonstrate uninterrupted polyhaline exposure between 16 and 19 August.

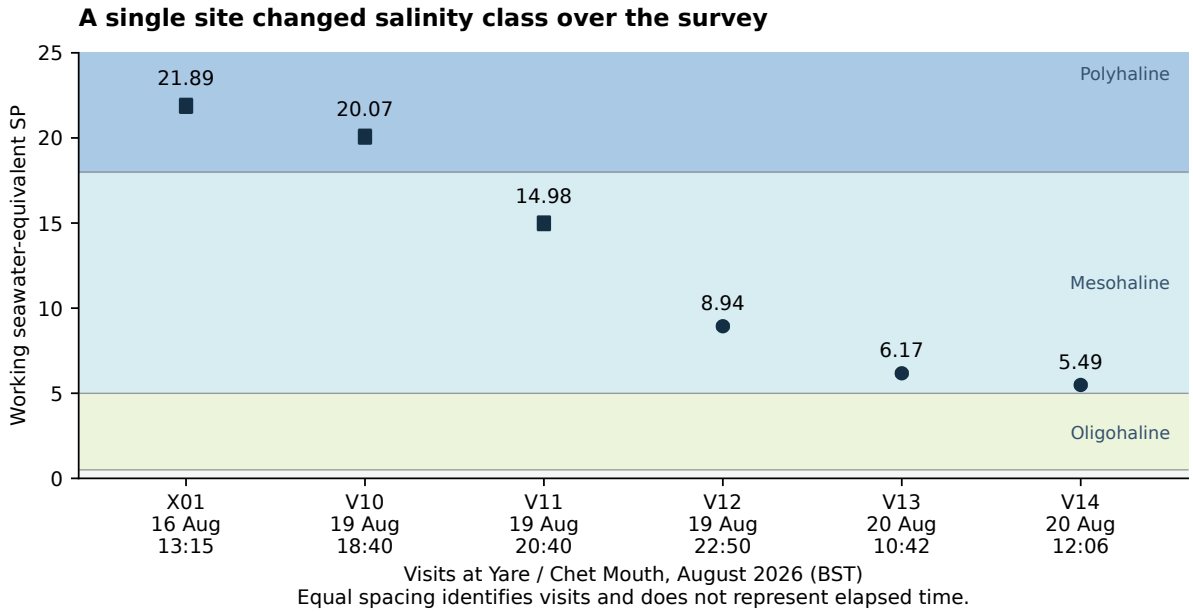


Figure 4: Six visits at Chet Mouth with conventional salinity bands. Symbols distinguish direct and dilution-derived observations; error bars are instrument specification endpoints. The categorical spacing identifies visits and does not represent elapsed time. No concentration is assigned to the gaps between observations.

4.4 Normal and drought expectations

Table 1 separates historical normal and drought expectations from field intensity. At Chet Mouth, the historical model-family drought P90 reaches approximately 15.01 mS cm^{-1}, well below X01's reconstructed 34.82. At Reedham the drought P90 reaches 16.51, compared with the field value 32.20. These large contrasts are departures from the modelled historical-calendar upper tails; they do not independently validate those tails under severe drought. The actual-time comparison remains a separate test because a particular combination of forcing may predict a value above the marginal drought P90.

Table 1: Selected normal and drought comparison summaries. Values are EC_{25} in mS cm^{-1} in the upper panel. Ranges span retained model variants; they are not confidence intervals. Lower-Yare drought tails are extrapolative and are not independently calibrated severe-drought quantiles. Oulton values are empirical sampled-date summaries. Lower-panel baselines use EA reported salinity (ppt), compared approximately with field S_{eq}. Full location coverage is in Appendix H.

Location	Normal median	Normal P90	Drought median	Drought P90
Chet Mouth	1.67 to 3.47	8.29 to 12.43	2.22 to 6.05	10.36 to 15.01
Reedham Reach	1.82 to 4.21	10.71 to 13.25	2.42 to 6.85	12.34 to 16.51
Coldham	0.85 to 0.86	0.95 to 1.01	0.92 to 0.93	1.00 to 1.06
Oulton Broad	2.40	2.84	Two drought dates: 4.02 and 6.78	
EA salinity station-model scale (reported ppt)				
Berney Arms	20.02	31.15	22.59	33.47
Burgh Castle	18.92	30.09	20.26	31.20

Oulton Broad demonstrates why salinity class and local unusualness must both be shown. Its oligohaline-equivalent observation is below the absolute salinity of the lower estuary, yet its direct conductivity of **8.030** mS cm^{-1} exceeds all 46 retained local native-EC25 station-days.

The archive maximum is 6.781 mS cm^{-1} on 6 September 2019, giving a central difference of 18.4%. The field instrument lower endpoint, 7.820, remains 15.3% above that recorded maximum; this calculation does not include historical instrument uncertainty, local spatial differences or unrecorded calibration bias (Figure 5). Only two native summer drought observations are available, 4.022 and 6.781; they cannot establish a reliable drought-tail percentile.

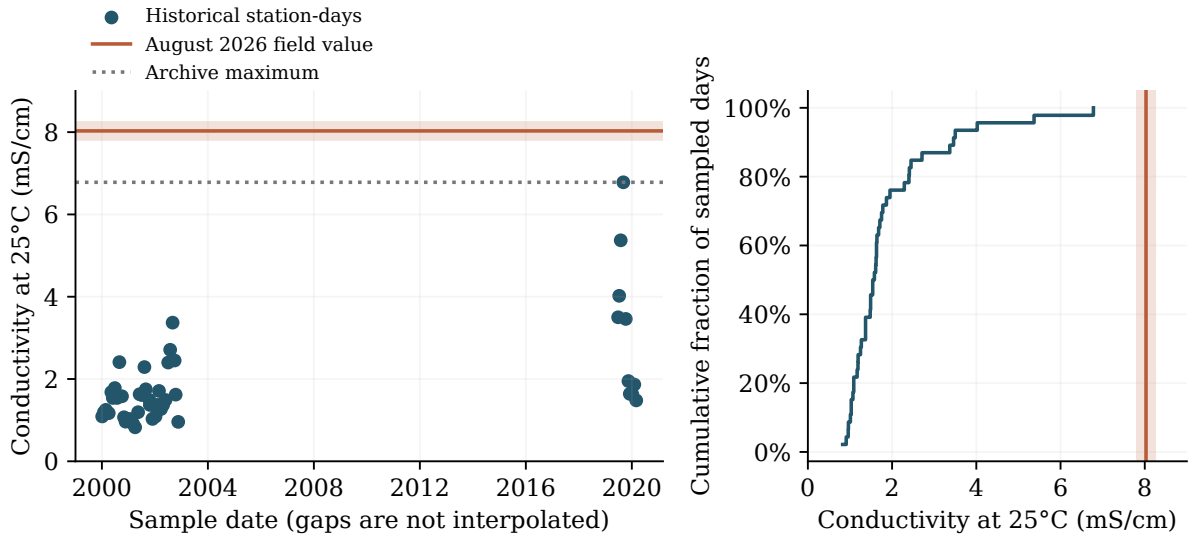


Figure 5: Oulton Broad compared with its local native-EC25 archive. The distribution is over 46 sampled station-days in five calendar years, not continuous monitoring over the full date span. The band around the field value is instrument-only.

The Oulton EC20 archive does not remove this contrast: its maximum converts to approximately 4.956 mS cm^{-1} in the nominal EC25 scenario and remains below the field lower endpoint after a separate 10% increase. The Broad station is approximately 77 m from the sample coordinate. Oulton Dyke values also exceed the Broad maximum, but the roughly 1.795 km spatial transfer is not validated and is not treated as an exact-site percentile.

At Herringfleet, the short native EC25 summer record at St Olaves gives a low historical comparator, but the separate EC20 summer P90 converts to approximately 19.642 mS cm^{-1}. All three Herringfleet values lie below it. The older method period therefore supplies important counter-evidence to a claim of historical exceptionalness. Near the estuary, observations at Berney Arms, Burgh Castle and the Waveney mouth have S_{eq} of 32.06, 30.79 and 31.01. They are euhaline but below the retained station-model drought P90s of 33.47 and 31.20 on the EA reported-ppt scale. Absolute intensity and statistical rarity do not rank sites in the same order.

4.5 Conditional departures and model limitations

At Chet Mouth on 16 August, X01's instrument-only lower endpoint of 34.225 mS cm^{-1} exceeds the largest primary summer sensitivity value, 33.490, by **0.735** mS cm^{-1}, approximately 2.1% of its central reconstructed value. This family includes tidal phase, response memory, flow reconstruction, omitted years and coastal-error tests. At Reedham on 19 August at 17:57, the corresponding margin is **1.867** mS cm^{-1}. These are exploratory departures within the specified summer comparison family (Table 3).

An idealised density-aware mixing scenario lowers X01's instrument endpoint from 34.225 to 33.915 mS cm^{-1} and V09's from 31.601 to 31.338. Their remaining summer-family margins are 0.425 and 1.604 respectively (Appendix B). Thus density weighting alone does not remove these departures, but the smaller Chet margin remains vulnerable to unquantified systematic

Table 2: Different evidence supports different claims. The rows are complementary, not independent statistical replications.

Evidence	Supported interpretation	Remaining boundary
Field observations	Saline surface water at the listed positions and times	No continuous plume, bottom profile or whole-month exposure record
Oulton local archive	Field conductivity exceeds the retrieved native-EC25 maximum	Sparse drought history and unquantified historical/local measurement differences
Chet and Reedham regression scenarios	Selected values exceed the specified summer sensitivity family	Severe-drought extrapolation and systematic conversion uncertainty; no calibrated event probability
Potential consequences	Mechanisms for habitat and water-use pressure	No measured ecological or agricultural damage and no event attribution

Table 3: Key conditional comparisons in $\mathrm{mS\,cm^{-1}}$ EC_{25}. Nominal is the largest actual-time P95 comparison across retained variants; summer is the primary summer sensitivity maximum. Margin is the field instrument lower endpoint minus summer. These are exploratory scenario comparisons, not calibrated exceedance probabilities or universal physical limits. The density sensitivity is reported separately in Appendix B.

Visit	Field	Lower	Nominal	Summer	Margin
Chet, 16 Aug 13:15	34.821	34.225	29.127	33.490	+0.735
Reedham, 19 Aug 17:57	32.198	31.601	27.673	29.734	+1.867
Chet, 19 Aug 18:40	32.198	31.601	30.693	31.926	-0.325
Coldham, 20 Aug 16:12	1.316	1.295	1.110	1.261	+0.034

measurement and comparator errors. The reference-seawater density assumption is a sensitivity, not a preferred empirical correction.

The native lower-Yare training cohort contains no summer drought response under the adopted definition. The conductivity bridge adds only 11 pooled summer drought responses, including three at Reedham and two at Chet Mouth. Approximately 91% of the native-model drought-calendar states are outside its joint flow training domain. Consequently, the X01 margin must be interpreted as a sensitivity-dependent model result rather than independent calibration of an extreme drought tail. Leaving the missing Tas hour unreconstructed and allowing its antecedent-state uncertainty to cover the entire historical driver range raises the X01 phase limit to $41.295\,\mathrm{mS\,cm^{-1}}$, which contains the observation. A different construction using the largest historical residual from any season reaches 65.513. This is not an all-season P95 and is not a typical drought expectation. Reedham survives the missing-Tas alternative, but its all-season maximum-error stress also contains the observation. Thus neither result is an assumption-free physical-bound violation.

Chet Mouth at 18:40 on 19 August remains a large historical contrast, but its instrument range overlaps the broader phase/state limit of $31.926\,\mathrm{mS\,cm^{-1}}$. The later Chet Mouth observations are contained by the conditional comparisons. The New Cut and nearby Yare visits can exceed nominal actual-time predictions while remaining inside phase sensitivities; their longer residual transfers are exploratory.

Coldham's direct $1.316\,\mathrm{mS\,cm^{-1}}$ exceeds its summer model comparisons but is accommodated by a broader all-month stress of 1.316443. Its marine-ion contribution is unresolved. Bramerton's 1.208 is within conditional expectations. Above Cantley, distance-weighted residual scenarios are exceeded, but transferring the endpoint residual law accommodates the observation. Loddon is high relative to its reviewed legacy marina comparator, while different-season logger peaks and spatial uncertainty prevent a validated local summer-drought claim. These limitations are

retained alongside the positive findings in the full location table (Appendix H).

An independent historical transfer diagnostic also rejects a candidate lower-Yare conductivity curve near Berney. Four shallow summer observations have a mean central underprediction of approximately 20.35 $\mathrm{mS\,cm^{-1}}$, and all 64 candidate variants underpredict on average. A wide prediction envelope does not repair this central bias. Accordingly, lower-estuary comparisons use the separate historical salinity station models and preserve their geographic and method qualifications.

5 Discussion

5.1 What the combined evidence establishes

The survey supports a spatially extensive, heterogeneous saline-water episode during the sampled part of August 2026. That statement rests on the conjunction of substantial seawater-equivalent salinity across connected reaches, repeated brackish observations and strong local historical contrasts. It does not require every observation to be an unprecedented value. The same-day 18.8 km endpoint spans on the Yare and Waveney, including 10.4 km between polyhaline-or-higher observations, give the pattern a scale that an isolated maximum cannot convey. A site-by-site table alone would obscure that result.

The strongest historical evidence has two different forms. Oulton Broad exceeds its retained local conductivity archive by a clear margin using a direct reading. Chet Mouth and Reedham exceed an extensive family of summer, flow- and tide-conditioned comparisons using reconstructed source-water conductivity. Oulton's sparse drought archive limits conditional probability claims; the Yare models have explicit measurement, spatial and severe-drought extrapolation limits. These findings are complementary. They support unusual conditions at important inland locations within a broader saline episode, while stopping short of a single validated probability for the entire event.

At the lower estuary, euhaline water can be compatible with historical drought expectations. At Oulton Broad, less saline water can be more exceptional relative to local history. The environmental meaning of an exposure also differs from its statistical rarity. A concentration that is expected in drought can still constrain freshwater habitat or water use. Conversely, a statistically elevated value near the low end of the conductivity range does not demonstrate a damaging marine incursion. Reporting class, historical context and potential exposure together avoids both errors.

5.2 Tides, flow and the freshening sequence

Tidal forcing has a material role in the analysis. On an identical historical cohort, adding the recorded high-water clock proxy to season, flow and depth reduced mean held-year absolute error from 5.95 to 4.19 on the EA salinity scale, a 29.6% improvement. Observed coastal forcing, alternative clocks, phase maxima and response-memory scenarios further test the field comparisons. The remaining uncertainty is not a failure to consider tides: it concerns how accurately the available predictors describe the local water mass and its history at a boat coordinate.

The Yare and regional flow indices satisfy the study drought rule throughout the survey, while Needham does not. That contrast is physically relevant rather than contradictory. Regional drought status and catchment runoff do not determine local tidal exchange in the same way, and Needham does not directly measure Oulton flushing. Salt transport depends on freshwater supply, tidal exchange, channel geometry and mixing [15]. A single catchment index cannot resolve every branch of this system.

At Chet Mouth, the marked decline during the evening of 19 August is consistent with displacement or dilution of saline surface water. Observed Reedham levels place the 22:50 sample

close to the approximately 23:00 level minimum; the 10:42 sample on 20 August is similarly close to the morning minimum near 10:45. These are water-level turning points, not demonstrated current slack or salinity minima. The reported overnight rain supplies another plausible influence, but rainfall, runoff timing and tidal transport were not independently separated. The observations therefore establish freshening, not its unique cause.

An estuary's response to a freshwater pulse depends on the preceding state and the pulse's intensity and duration [4]. Here, reported rainfall was not converted into an independently measured local discharge pulse, so this mechanism does not identify the cause of freshening.

5.3 Channel shape, drainage and vertical structure

Channel geometry can modify transport, storage and mixing even under similar river and coastal forcing [5, 15]. The Pamlico experiments show that topographic constraints can limit seasonal salt-front migration while salinity increases under sea-level rise [37]. This is a reason to retain branch-specific interpretation in the Broads. River distance and statistical interactions do not replace bathymetry, a salt balance or independently observed exchange through side waters. The present models do not identify how much of any local departure is attributable to channel shape.

Drainage and water management can also change the relation between gauged freshwater inflow and local salt exposure. A combined historical and palaeolimnological study of Hickling and Martham Broads links changes in plant salinity tolerance to probable drainage modifications [30]. Those Thurne-valley findings establish relevant regional context, not a measured explanation for the southern Broads observations. Pumping, abstraction and gate or lock operation remain possible influences here. Quantifying their contributions would require time-matched operation and discharge records, local geometry and salinity observations that resolve exchange. No such causal separation is claimed.

Surface sampling has a precise interpretation. It shows that saline water reached the sampled upper layer near the river centre and was not documented only in an isolated bottom layer. In a stratified estuary, bottom water may be more saline, but the vertical gradient here was not measured. Nor is there evidence that every historical EA comparator was collected deeper. Idealised experiments show that stratification can itself alter tidal propagation by changing turbulence and friction [29]. Thus local tidal forcing and vertical structure need not be independent. This result does not supply a Broads-specific depth correction. No automatic correction or evidential multiplier is applied for presumed depth differences, and the survey cannot establish the total salt inventory or its persistence near the bed.

5.4 What models add, and what they cannot yet resolve

The models translate disjoint historical samples into explicit working normal, drought and visit-conditioned expectations. Their usefulness is demonstrated by withheld-year performance, their sensitivity to tide information and the ability to test an observation against more adverse forcing or residual scenarios. Reporting both central expectations and upper comparisons is more informative than treating an exceedance of a marginal P90 as sufficient proof of a forcing-adjusted anomaly.

Comparable modelling studies clarify the level of evidence needed for further development. The Scheldt study used long daily salinity records and spatially resolved catchment runoff [38]. Its daily-mean target differs from a sample at a particular tidal phase. A confidence interval for a long-term mean or mean front position also answers a different question from a prediction interval for an individual field observation. More complex models could use richer local data, but their published accuracy or interval widths cannot be transferred to this survey.

Cong and colleagues withheld the full 2025 dry season and calibrated forecast intervals using development-period residuals [9]. That design supports evaluation on an untrained season, while leaving transfer to other sites unresolved. The corresponding priority here is independent

local drought episodes for checking both central predictions and upper-tail coverage. Increasing algorithmic complexity alone would not resolve the present lack of such observations.

The largest remaining limitation is the historical response population under comparably severe drought. The native lower-Yare conductivity cohort contains no summer drought responses under the fixed classification. The supplementary method bridge adds only 11 pooled summer drought responses, including three at Reedham and two at Chet Mouth. Many modelled drought-calendar states lie outside the joint flow range used for fitting. Wider error envelopes expose sensitivity, but they do not create independent severe-drought observations or calibrate a tail probability. The positive summer comparisons should therefore be read as model-supported evidence with stated scope, not as precise return periods.

The analysis also retains negative evidence. Response-memory variants did not improve average withheld-year error, the candidate Berney conductivity transfer failed an independent shallow-water check and historical EC20 observations weaken an exceptionalness claim at Herringfleet. These outcomes guard against selecting only models that make the field survey appear extreme. Field salinity was withheld from historical fitting. Nevertheless, model development and the choice of sensitivity questions were informed by this episode, so the work remains an exploratory case study rather than a preregistered confirmatory test. Multiple visits are dependent and their exceedances are not multiplied into a small event probability.

The broadest algebraic stresses can accommodate even the largest inland observations. They are useful for identifying assumptions that control the conclusion, but a maximum residual from any season is not a typical drought expectation. The defensible interpretation separates three claims: saline surface water was measured across connected reaches; some observations exceed a retrieved local archive or a specified model comparison; the probability of such observations under comparable historical drought is not calibrated. An unrestricted stress envelope does not establish ordinary conditions, but a smaller selected envelope does not establish a universal upper limit either.

5.5 Alternative explanations and evidence that could change the conclusion

The direct Oulton contrast would weaken if comparable historical records contained higher values, if documented calibration bias accounted for the difference or if matched measurements showed a persistent local difference between the sample and archive positions. The Chet Mouth and Reedham model departures would weaken if independent severe-drought episodes showed that the transferred residual distribution understated the upper tail, or if measurement-model corrections removed their small remaining margins. Conversely, sustained excesses in independently withheld, depth- and tide-matched drought records would strengthen a conditional anomaly claim. These are testable alternatives rather than assumed explanations.

Shared meter bias or a shared conversion assumption could affect several observations together. Spatial extent and agreement across dilution ratios do not eliminate that possibility. The archive's irregular sampling could also have missed historical peaks. The survey's surface observations establish exposure in the sampled layer, but neither an unusually long saline-front reach relative to earlier droughts nor a trend in the frequency of such episodes has been estimated. These limits remain even if every listed calculation is reproduced exactly.

5.6 Potential consequences of repeated exposure

The spatial footprint matters for management because water users and aquatic organisms depend on connected waterways. If saline conditions extend across several reaches at once, the availability of fresher water nearby may decrease. The moving survey does not establish simultaneous refuge loss, but it identifies why continuous observations across the connected network would be more useful than isolated maxima.

For agriculture, relevant mechanisms include osmotic stress, ion accumulation and, where sodium chemistry is unfavourable, soil-structure effects. Irrigation guidance uses conductivity alongside crop, soil, drainage and management conditions [2]. If water from affected reaches is abstracted for irrigation, suitable intake periods may narrow and stored freshwater or blending may become more valuable. These are conditional implications. The study contains no records of abstraction, irrigation application, crop exposure, soil sodium or yield. River conductivity must not be equated with soil salinity or with demonstrated agricultural loss.

For fisheries and freshwater ecosystems, prolonged or repeated exposure could change habitat suitability, movement opportunities, reproduction and community composition. The Broads Authority identifies saline incursions as a risk to freshwater plants, fish and invertebrates [8]. Experimental freshwater research also shows that salinisation can alter food webs, although road-salt experiments are not a calibrated response model for Broads seawater incursions [17]. Species tolerance, life stage, temperature, oxygen and exposure duration matter. Naturally brackish habitats should not be treated as intrinsically degraded. At Hickling and Martham, sedimentary plant remains reveal saline conditions not captured fully by historical plant records, including the presence of a conservation-relevant brackish-water species [30]. That evidence reinforces the distinction between exceeding a short monitoring archive and exceeding all past conditions. It also shows why ecological interpretation must respect each waterbody's history. This survey recorded neither fish mortality nor ecological damage.

The Chet Mouth sequence is especially relevant to exposure assessment: a high reading can fall substantially within hours. Conversely, repeated Oulton and Herringfleet observations show why a single later low measurement cannot describe the whole sampled episode. Continuous salinity, temperature and oxygen records, linked to biological observations and actual water use, would turn potential consequences into testable local impact assessments.

5.7 Climate context without event attribution

Climate projections provide a reason to take recurring saline exposure seriously. UK projections indicate a greater likelihood of drier summers, with marked summer drying in southern England [24]. A multi-hydrological-model study projects worsening river-flow drought in most assessed UK catchments, conditional on its high-emissions scenario and climate-model family; groundwater responses are less uniform [26]. Marine projections show rising mean sea level, without requiring a significant additional increase in atmospheric storm-surge forcing [23].

A study of 18 estuaries under SSP3-7.0 projects increased intrusion in most systems under combined discharge and sea-level change [21]. It supplies context for the direction of concern, not a Broads-specific recurrence forecast. The Pamlico study adds a conditional seasonal perspective: stronger discharge contrasts can enlarge salt-front migration, whereas greater sea-level rise can constrain that migration through local topography even as intrusion increases [37]. A general expectation of greater salinity pressure therefore need not imply a uniform increase in seasonal front movement at every site. These studies address other estuaries and do not independently validate the August 2026 comparisons.

Combining those projections with estuarine transport physics suggests that reduced freshwater flushing and higher coastal levels could allow saline water to reach farther inland or persist longer. This is a mechanistic inference, not a result of a future simulation in this study. Channel change, abstraction, gates, locks and other management can modify the response. The data do not quantify how often an August-2026-like episode will recur or attribute this episode to anthropogenic climate change.

A claim that UK drought frequency has already increased would require a separate trend analysis using a fixed definition and long homogeneous records. Historical reconstructions show that severe earlier droughts may be absent from short modern monitoring series [3]. Neither the regional declaration nor this field campaign can establish a national trend. The defensible prospective concern is increasing salinity pressure under plausible future low-flow and sea-level

conditions, with consequences that depend on exposure and local vulnerability.

5.8 Evidence that would most improve the answer

The priority is independent local summer drought salinity with matched flow, tide, timestamp and depth. Whole drought episodes could then be withheld to assess conditional upper-tail coverage. Paired measurements at field and comparator locations would test spatial transfer, especially near Reedham and the lower Yare. A local Oulton salinity and water-exchange record would establish whether the archive exceedance is also unusual under comparable drought and lock conditions. Confirmed reference-temperature settings and independent conductivity, chloride or salinity checks would narrow the measurement-model uncertainty.

These are specific routes to stronger conclusions, not prerequisites for reporting the present evidence. Appendix I identifies the variables, possible custodians, analysis operations and benefits. No further field observations are assumed in the current study. Existing-data results remain reportable at their stated level: sampled concentrations and extent, historical archive contrasts and qualified model-conditioned departures.

6 Conclusion

The survey documented saline surface water across substantial connected reaches during 16 to 20 August 2026. On 19 August, mesohaline-or-higher observations span approximately 18.8 km between endpoints on the Yare and Waveney, including 10.4 km between polyhaline-or-higher observations. These measurements describe sampled concentrations and geographical spread, not a continuously measured plume or the length proven historically anomalous.

The answer to whether salinity exceeded historical drought expectations differs by location and evidential basis. Oulton Broad exceeds the retrieved local conductivity archive, but too few matched drought observations are available to estimate its conditional rarity. Chet Mouth and Reedham exceed the specified summer regression sensitivity family under the working measurement conversion. Sparse severe-drought validation, spatial transfer and systematic measurement assumptions prevent treating those departures as calibrated tail probabilities. Broader error scenarios contain them. Some lower-estuary readings are compatible with modelled drought expectations and several other sites have no validated local drought baseline.

The study's contribution is an August 2026 southern Broads surface-water case with traceable observations, local historical contrasts and explicit drought-conditioned comparison limits. It supports a geographically extensive saline surface-water pattern with particular local historical and exploratory model departures. It does not establish that the entire sampled network, or August as a whole, was exceptionally saline after all forcing had been accounted for. Repeated exposure could constrain freshwater habitats, fisheries and water use under future low-flow and sea-level changes, making exposure duration and access to fresher water important management questions. Channel shape, drainage management and vertical stratification are plausible modifiers that remain unresolved locally. Agricultural or ecological damage and attribution to anthropogenic climate change were not measured.

Data, code and declarations

Data and code. The analytical archive contains the original investigator-supplied workbook, the 36-row field register, comparison and validation tables, plotting inputs, executable reproduction checks and the LaTeX and BibTeX sources. It distinguishes calculations regenerated from frozen inputs from historical outputs retained for inspection. Appendix J defines that boundary. A separate public supplement preserves provider-specific terms. It omits NRFA daily-flow inputs and detailed numerical flow predictors because their download terms require agreement for online

redistribution. Readers obtain these inputs directly from NRFA under its terms; the supplement provides provenance, schemas and preparation code. Eligible historical chemistry, coastal features, model coefficients and research results are retained. No public repository accession or DOI has yet been assigned.

Research capacity and acknowledgements. Michael Natusch collected the field observations and undertook the study as an independent researcher. The Environment Agency and the Broadland Futures Initiative supplied the HR Wallingford report. This acknowledgement does not imply their endorsement. The report and private correspondence are not redistributed. Data from the UK National River Flow Archive. Contains Environment Agency information licensed under the Open Government Licence v3.0. Historical coastal information was obtained through GESLA and the University of Hawaii Sea Level Center, with BODC identified as the originating provider. These sources retain their own terms and attribution. No human-participant research or animal experiment was performed.

Funding. This research received no funding.

Competing interests. The author declares no competing interests.

Author approval. The author has reviewed and approved the science, references, data and code and takes responsibility for the work. Informal discussions with practising scientists do not constitute journal peer review.

Manuscript licence. Copyright © 2026 Michael Natusch. This manuscript is licensed under the Creative Commons Attribution 4.0 International licence (CC BY 4.0): `https://creativecommons.org/licenses/by/4.0/`. Third-party source data retain their own terms and are not relicensed by this statement. The map contains OpenStreetMap data, © OpenStreetMap contributors, available under the Open Database Licence: `https://www.openstreetmap.org/copyright`.

Declaration of generative AI and AI-assisted technologies

During this work, the author used OpenAI ChatGPT/Codex for literature retrieval, data processing, code generation, model specification and implementation, figure preparation, numerical checking and manuscript drafting. This assistance was not limited to copyediting. After using these tools, the author reviewed and approved the science, references, data and code and accepts full responsibility for the content. Methods describes the reproducible numerical and visualisation workflow. Exact AI model identifiers for all historical sessions were not retained and are not reconstructed retrospectively; the supplement records the numerical software environment and executable checks. AI systems are not authors. Computational checks within the same AI-assisted workflow do not constitute independent scientific validation on a new drought event. The manuscript has not undergone journal peer review.

References

[1] Apera Instruments (Europe) GmbH. *EC20 Pocket Conductivity Tester: Instruction Manual*. Apera Instruments (Europe) GmbH, 2.2 edition, n.d. URL `https://aperainst.de/wp-content/uploads/2020/09/EC20-EN-3.pdf`. Accessed 11 September 2026. Sections 6 to 8; publication date not stated.

[2] R. S. Ayers and D. W. Westcot. Water quality for agriculture. Technical Report 29 Rev. 1, Food and Agriculture Organization of the United Nations, Rome, 1985. URL `https://www.fao.org/4/t0234e/T0234E01.htm`. Chapter 1, Table 1 and accompanying assumptions.

[3] Lucy J. Barker, Jamie Hannaford, Simon Parry, Katie A. Smith, Maliko Tanguy, and Christel Prudhomme. Historic hydrological droughts 1891 to 2015: systematic characterisation for a diverse set of catchments across the UK. *Hydrology and Earth System Sciences*, 23:4583 to 4602, 2019. doi: 10.5194/hess-23-4583-2019. URL `https://hess.copernicus.org/articles/23/4583/2019/`.

[4] Bouke Biemond, Huib E. de Swart, Henk A. Dijkstra, and Manuel Díez-Minguito. Estuarine salinity

response to freshwater pulses. *Journal of Geophysical Research: Oceans*, 127(11):e2022JC018669, 2022. doi: 10.1029/2022JC018669. URL https://doi.org/10.1029/2022JC018669.

[5] Bouke Biemond, Wouter M. Kranenburg, Ymkje Huismans, Huib E. de Swart, and Henk A. Dijkstra. Dynamics of salt intrusion in complex estuarine networks: an idealised model applied to the Rhine-Meuse Delta. *Ocean Science*, 21:261 to 281, 2025. doi: 10.5194/os-21-261-2025. URL https://doi.org/10.5194/os-21-261-2025.

[6] British Oceanographic Data Centre. UK Tide Gauge Network: Data access and quality control. National Oceanography Centre data service, 2026. URL https://www.bodc.ac.uk/data/hosted_data_systems/sea_level/uk_tide_gauge_network/. Accessed 11 September 2026.

[7] Broads Authority. Facts and figures, n.d.. URL https://www.broads-authority.gov.uk/about-the-broads/facts-and-figures. More than 125 miles (200 km) of navigable rivers and broads; accessed 11 September 2026.

[8] Broads Authority. Issues affecting lakes and SSSI condition. Technical report, Broads Authority, n.d.. URL https://www.broads-authority.gov.uk/__data/assets/pdf_file/0027/106983/Appendix_1_Issues_affecting_lakes-1.pdf. Appendix 1 to the Broads Lake Restoration Strategy; climate change and saline incursion discussion, PDF p. 7. Publication date not stated in the supplied appendix.

[9] Nguyen Phuoc Cong, Nigel K. Downes, Huynh Vuong Thu Minh, and Pankaj Kumar. Multi-day salinity forecasting in the Vietnamese Mekong Delta: Horizon-dependent performance and interpretation of XGBoost, LSTM, and a weighted hybrid. *Water*, 18(19):2379, 2026. doi: 10.3390/w18192379. URL https://doi.org/10.3390/w18192379. Published 24 September 2026.

[10] Department for Environment, Food & Rural Affairs and Environment Agency. Drought declared in half of england. GOV.UK press release, 29 July 2026, 2026. URL https://www.gov.uk/government/news/drought-declared-in-half-of-england. Accessed 11 September 2026. East Anglia is explicitly included in the declared areas.

[11] Environment Agency. Hydrology data API: Reference documentation. Online data service, 2026. URL https://environment.data.gov.uk/hydrology/doc/reference. Accessed 11 September 2026. Historical and recent flow, level, rainfall and water-quality time series.

[12] Environment Agency. Water Quality Explorer: Public API documentation. Online data service, 2026. URL https://environment.data.gov.uk/water-quality/api-docs. Accessed 11 September 2026. Data subject to the Open Government Licence v3.0.

[13] Environment Agency Hydrology Team. East anglia water situation: July 2026 summary. GOV.UK, updated 12 August 2026, 2026. URL https://www.gov.uk/government/publications/water-situation-local-area-reports/east-anglia-water-situation-july-2026-summary. Accessed 11 September 2026. Provisional hydrological data.

[14] Federal Geographic Data Committee. Coastal and marine ecological classification standard. Technical Report FGDC-STD-018-2012, Federal Geographic Data Committee, June 2012. URL https://coast.noaa.gov/data/digitalcoast/pdf/cmecs.pdf. Section 5.2 and Table 5.2, pp. 39 to 40; freshwater system definitions in Section 4.2.2.

[15] W. Rockwell Geyer and Parker MacCready. The estuarine circulation. *Annual Review of Fluid Mechanics*, 46:175 to 197, 2014. doi: 10.1146/annurev-fluid-010313-141302. URL https://doi.org/10.1146/annurev-fluid-010313-141302.

[16] Ivan D. Haigh, Marta Marcos, Stefan A. Talke, Philip L. Woodworth, John R. Hunter, Ben S. Hague, Arne Arns, Elizabeth Bradshaw, and Philip Thompson. GESLA version 3: A major update to the global higher-frequency sea-level dataset. *Geoscience Data Journal*, 10(3):293 to 314, 2023. doi: 10.1002/gdj3.174. URL https://doi.org/10.1002/gdj3.174. First published online 8 September 2022.

[17] William D. Hintz, Brian M. Mattes, Matthew S. Schuler, Devin K. Jones, Aaron B. Stoler, Lovisa Lind, and Rick A. Relyea. Salinization triggers a trophic cascade in experimental freshwater communities with varying food-chain length. *Ecological Applications*, 27:833 to 844, 2017. doi: 10.1002/eap.1487. URL https://doi.org/10.1002/eap.1487.

[18] HR Wallingford. Statistical modelling of saline intrusions. Final report, Product 25d DER7003-RT001 R07-00, Broadland Futures Initiative, 2025. 14 March 2025, 94 pp. Final report supplied to the

author by the Environment Agency on 7 September 2026; no public download URL verified.

[19] IOC, SCOR, and IAPSO. The international thermodynamic equation of seawater 2010: Calculation and use of thermodynamic properties. Manuals and Guides 56, UNESCO, Intergovernmental Oceanographic Commission, 2010. URL https://www.teos-10.org/pubs/TEOS-10_Manual.pdf. 196 pp.; Appendix E describes Practical Salinity.

[20] Zheng Kang, Hanliang Huang, Jingwen Zhang, Zejun Li, Yifan Chen, Boheng Du, Kairong Lin, and Xiaohong Chen. Estuarine salinity prediction using empirical mode decomposition and random forest for supporting water resource management. *Scientific Reports*, 16(1):17497, 2026. doi: 10.1038/s41598-026-48012-5. URL https://www.nature.com/articles/s41598-026-48012-5.pdf. Article 17497, published 15 April 2026.

[21] Jiyong Lee, Bouke Biemond, Daan van Keulen, Ymkje Huismans, René M. van Westen, Huib E. de Swart, Henk A. Dijkstra, and Wouter M. Kranenburg. Global increases of salt intrusion in estuaries under future environmental conditions. *Nature Communications*, 16:3444, 2025. doi: 10.1038/s41467-025-58783-6. URL https://doi.org/10.1038/s41467-025-58783-6.

[22] Trevor McDougall and Paul Barker. gsw_SP_from_C: Practical salinity from conductivity. Gibbs SeaWater Oceanographic Toolbox documentation, version 3.05, 2015. URL https://www.teos-10.org/pubs/gsw/html/gsw_SP_from_C.html. Documentation dated 16 February 2015; accessed 11 September 2026. The analysis used the separately recorded Python package version.

[23] Met Office. UKCP18 factsheet: Sea level rise and storm surge. Technical report, Met Office, November 2025. URL https://www.metoffice.gov.uk/api/assets/file/ukcp18-sea-level-rise-storm-surge-factsheet-november-2025pdf?prefix=assets. Updated November 2025.

[24] Met Office. UKCP18 factsheet: Precipitation. Technical report, Met Office, January 2026. URL https://www.metoffice.gov.uk/api/assets/file/ukcp18-precipitation-factsheet-january-2026pdf?prefix=assets. Updated January 2026.

[25] OpenStreetMap contributors. Waterway centreline data, 2026. URL https://www.openstreetmap.org/copyright. Open Database Licence; frozen waterway extract and routing details supplied with the analytical supplement.

[26] Simon Parry, Jonathan D. Mackay, Thomas Chitson, Jamie Hannaford, Eugene Magee, Maliko Tanguy, Victoria A. Bell, Katie Facer-Childs, Alison Kay, Rosanna Lane, Robert J. Moore, Stephen Turner, and John Wallbank. Divergent future drought projections in UK river flows and groundwater levels. *Hydrology and Earth System Sciences*, 28:417 to 440, 2024. doi: 10.5194/hess-28-417-2024. URL https://hess.copernicus.org/articles/28/417/2024/.

[27] Rich Pawlowicz. Calculating the conductivity of natural waters. *Limnology and Oceanography: Methods*, 6(9):489 to 501, 2008. doi: 10.4319/lom.2008.6.489. URL https://doi.org/10.4319/lom.2008.6.489.

[28] David R. Roberts, Volker Bahn, Simone Ciuti, Mark S. Boyce, Jane Elith, Gurutzeta Guillera-Arroita, Severin Hauenstein, José J. Lahoz-Monfort, Boris Schröder, Wilfried Thuiller, David I. Warton, Brendan A. Wintle, Florian Hartig, and Carsten F. Dormann. Cross-validation strategies for data with temporal, spatial, hierarchical, or phylogenetic structure. *Ecography*, 40(8):913 to 929, 2017. doi: 10.1111/ecog.02881. URL https://doi.org/10.1111/ecog.02881. First published online 8 December 2016.

[29] R. W. A. Siemes and S. J. M. H. Hulscher. Salinity-induced stratification impacts tides in estuaries. *Advances in Water Resources*, 215:105388, 2026. doi: 10.1016/j.advwatres.2026.105388. URL https://doi.org/10.1016/j.advwatres.2026.105388. First published online 24 June 2026.

[30] N. J. B. Stommel, L. R. Roberts, T. A. Davidson, A. L. Jourdan, and D. J. Hoare. Combining historical records and palaeolimnology to reconstruct changes in aquatic macrophyte communities in shallow, brackish lakes: A Norfolk Broads case study. *Aquatic Conservation: Marine and Freshwater Ecosystems*, 36(2):e70347, 2026. doi: 10.1002/aqc.70347. URL https://doi.org/10.1002/aqc.70347.

[31] TEOS-10. gsw_rho_t_exact: in-situ density of seawater, 2015. URL https://www.teos-10.org/pubs/gsw/html/gsw_rho_t_exact.html. Function documentation, version 3.05; accessed 24 September 2026.

[32] TEOS-10. gsw_SR_from_SP: Reference salinity from practical salinity, 2015. URL https://www.teos-10.org/pubs/gsw/html/gsw_SR_from_SP.html. Function documentation, version 3.05; accessed 24 September 2026.

[33] UK Centre for Ecology & Hydrology. National River Flow Archive: NRFA API. Online data service, 2026. URL https://nrfa.ceh.ac.uk/data/use-nrfa-data/nrfa-api. Accessed 11 September 2026. Data from the UK National River Flow Archive.

[34] UNESCO. The Practical Salinity Scale 1978 and the International Equation of State of Seawater 1980. Technical Papers in Marine Science 36, UNESCO, 1981. URL https://www.teos-10.org/pubs/gsw/pdf/SP_from_C.pdf. 25 pp. Bibliographic details and the implemented algorithm are documented in the official GSW notes.

[35] University of Hawaii Sea Level Center. GESLA sea level (sub-hourly to hourly): ERDDAP dataset and metadata. Dataset global_hourly_gesla, 2026. URL https://uhslc.soest.hawaii.edu/erddap/info/global_hourly_gesla/index.html. Metadata creation date 20 July 2026. Accessed 11 September 2026; record-specific quality flags and source providers retained.

[36] Tess M. Wegman, Julie D. Pietrzak, Alexander R. Horner-Devine, Henk A. Dijkstra, and David K. Ralston. Observations of estuarine salt intrusion dynamics during a prolonged drought event in the Rhine-Meuse Delta. *Journal of Geophysical Research: Oceans*, 130(1):e2024JC021655, 2025. doi: 10.1029/2024JC021655. URL https://doi.org/10.1029/2024JC021655. First published online 25 December 2024.

[37] Dongxiao Yin, Courtney Kay Harris, Duc Tran, Mahesh R. Tapas, Venkataraman Lakshmi, Michael A. O'Driscoll, and Stephen Moysey. Saltwater intrusion seasonality under climate change: Interacting effects of river discharge, sea-level rise, and bathymetry. *Geophysical Research Letters*, 53(21):e2026GL122717, 2026. doi: 10.1029/2026GL122717. URL https://doi.org/10.1029/2026GL122717. First published online 5 November 2026.

[38] Boli Zhu, Danitza Salazar, and Patrick Willems. Long-term daily salinity prediction in a tidal estuary using coupled machine learning and physically-based models. *Journal of Hydrology: Regional Studies*, 67:103838, 2026. doi: 10.1016/j.ejrh.2026.103838. URL https://doi.org/10.1016/j.ejrh.2026.103838.

A Field register

The analytical register contains 36 quantified observations. Stable identifiers link the tables to the companion CSVs and figures; identifiers are not consecutive sampling numbers. The original display values, preparation ratios and tap conductivities are retained. No value is excluded merely because it exceeds an expected seawater equivalent. Latitude and longitude use decimal degrees. V20 remains at its submitted coordinate without an inferred waterbody. These records define the study population and all 36 appear in the spatial and class summaries.

Table 4: Field locations and times. Dates are in August 2026 and times are BST. All river observations represent surface water close to the river centre. Labels are descriptive and the coordinates remain authoritative.

ID	Day and time	Location	Latitude	Longitude
X01	16, 13:15	Yare at Chet Mouth	52.55588	1.53982
X02	16, 18:50	Waveney at Herringfleet moorings	52.52631	1.62884
X03	17, 12:30	Waveney at Herringfleet moorings	52.52631	1.62884
X04	17, 16:15	Waveney at Beccles Quay	52.46504	1.56415
X05	17, 17:03	Waveney at Beccles Quay	52.46504	1.56415
X06	18, 12:43	Waveney at52.46223,1.62943	52.46223	1.62943
X07	18, 15:08	Oulton Broad	52.47476	1.70797
X08	18, 16:38	Oulton Dyke	52.47682	1.68165
X09	18, 19:22	Oulton Dyke	52.47682	1.68165
X10	18, 22:36	Oulton Dyke	52.47682	1.68165
X11	19, 10:55	Oulton Dyke	52.47682	1.68165
X12	19, 12:16	Waveney at Herringfleet moorings	52.52631	1.62884
X13	19, 12:22	Waveney north of Herringfleet	52.53166	1.62139
X14	19, 13:04	Yare near Reedham, eastern visit	52.55858	1.57389
X15	19, 13:39	Yare near Reedham, western visit	52.55929	1.56752
V02	19, 13:54	Yare at New Cut junction	52.55678	1.57909
V03	19, 14:33	Lower Yare near Berney Arms	52.58238	1.63716
V04	19, 16:37	Waveney at Burgh Castle	52.57552	1.64793
V05	19, 16:51	Lower Waveney near its mouth	52.58808	1.64653
V06	19, 17:04	Lower Yare west of Berney Arms	52.58056	1.62904
V07	19, 17:21	Seven Mile Reach	52.56866	1.60695
V08	19, 17:38	Yare at New Cut junction	52.55663	1.57882
V09	19, 17:57	Reedham Ferry Reach	52.55625	1.54679
V10	19, 18:40	Yare at Chet Mouth	52.55590	1.53975
V11	19, 20:40	Yare at Chet Mouth	52.55590	1.53975
V12	19, 22:50	Yare at Chet Mouth	52.55590	1.53975
V13	20, 10:42	Yare at Chet Mouth	52.55588	1.53976
V14	20, 12:06	Yare at Chet Mouth	52.55588	1.53976
V15	20, 12:33	Lower River Chet	52.55289	1.53918
V16	20, 13:01	Chet at Church Farm	52.54086	1.51166
V17	20, 13:31	Chet at Loddon	52.53886	1.48776
V18	20, 15:06	Yare above Cantley	52.57570	1.49253
V19	20, 15:36	Fleet Dyke	52.59865	1.45158
V20	20, 15:45	Unassigned 15:45 coordinate	52.57848	1.43802
V21	20, 16:12	Coldham Hall Reach	52.61075	1.43611
V22	20, 20:44	Bramerton Reach	52.60540	1.38262

Table 5: Measurements and derived values. Display and tap values have been expressed in $\mathrm{mS\,cm^{-1}}$; the original displayed unit is retained in the CSV. R:T is river:tap volume ratio and 1:0 denotes undiluted water. Temperature is the meter reading in °C. EC_{25} is the working source-water equivalent.

ID	Display	Temp.	R:T	Tap	EC_{25}	S_{eq}	Instrument S_{eq}
X01	13.280	23.9	1:2	1.0500	34.821	21.89	21.47 to 22.30
X02	7.260	23.5	1:2	1.0640	18.460	10.92	10.53 to 11.31
X03	6.040	21.8	1:2	0.0954	16.624	9.75	9.36 to 10.13
X04	1.093	22.2	1:0	n/a	1.093	0.54	0.53 to 0.55
X05	1.086	21.6	1:0	n/a	1.086	0.54	0.53 to 0.55
X06	1.478	21.9	1:0	n/a	1.478	0.74	0.73 to 0.75
X07	8.030	22.0	1:0	n/a	8.030	4.45	4.32 to 4.57
X08	8.130	21.6	1:0	n/a	8.130	4.50	4.38 to 4.63
X09	7.600	21.4	1:0	n/a	7.600	4.19	4.07 to 4.31
X10	7.630	21.4	1:0	n/a	7.630	4.21	4.08 to 4.33
X11	7.630	21.2	1:0	n/a	7.630	4.21	4.08 to 4.33
X12	15.190	21.2	1:0	n/a	15.190	8.84	8.70 to 8.97
X13	16.290	23.0	1:0	n/a	16.290	9.53	9.40 to 9.67
X14	9.770	22.0	1:2	1.0870	25.279	15.39	14.99 to 15.79
X15	9.800	22.3	1:2	1.1970	25.190	15.33	14.93 to 15.73
V02	10.810	23.1	1:2	1.1970	27.933	17.17	16.76 to 17.58
V03	14.590	23.9	1:3	1.1970	49.075	32.06	31.50 to 32.62
V04	14.010	23.6	1:3	1.0760	47.340	30.79	30.23 to 31.35
V05	14.100	23.3	1:3	1.0760	47.649	31.01	30.46 to 31.57
V06	16.380	22.2	1:3	1.0760	55.440	36.77	36.20 to 37.33
V07	13.410	21.6	1:3	1.0760	45.274	29.29	28.74 to 29.85
V08	9.750	22.4	1:3	1.0760	32.538	20.31	19.77 to 20.85
V09	12.310	22.4	1:2	1.0580	32.198	20.07	19.66 to 20.48
V10	12.310	22.3	1:2	1.0580	32.198	20.07	19.66 to 20.48
V11	9.530	21.4	1:2	1.0580	24.671	14.98	14.58 to 15.39
V12	15.350	21.9	1:0	n/a	15.350	8.94	8.81 to 9.07
V13	10.900	21.4	1:0	n/a	10.900	6.17	6.05 to 6.30
V14	9.770	21.7	1:0	n/a	9.770	5.49	5.36 to 5.61
V15	10.370	21.4	1:0	n/a	10.370	5.85	5.72 to 5.98
V16	11.330	20.6	1:0	n/a	11.330	6.44	6.31 to 6.57
V17	5.610	19.3	1:0	n/a	5.610	3.03	2.91 to 3.15
V18	3.950	21.1	1:0	n/a	3.950	2.09	1.97 to 2.20
V19	1.479	21.6	1:0	n/a	1.479	0.74	0.73 to 0.75
V20	1.364	21.2	1:0	n/a	1.364	0.68	0.67 to 0.69
V21	1.316	20.9	1:0	n/a	1.316	0.66	0.64 to 0.67
V22	1.208	20.8	1:0	n/a	1.208	0.60	0.59 to 0.61

B Measurement conversion and sensitivity

The calculation uses Python GSW version 3.6.23. For each displayed conductivity and tap control, `SP_from_C(C,25,0)` produces a seawater equivalent. Equation 1 reconstructs the source equivalent and `C_from_SP(S,25,0)` returns its EC_{25} equivalent. The use of 25 °C is an explicit reference-setting assumption, not the measured vessel temperature. Temperature compensation must not be applied twice.

For the instrument lower endpoint, mixture conductivity is decreased by its specification allowance and tap conductivity increased by its allowance. The upper endpoint reverses those choices. Tap values are bounded at zero where necessary. Precisely measured dilution ratios are retained without an invented random volume uncertainty. The endpoint interval therefore covers

only the stated meter specification within the adopted conversion model. Composition, density and calibration effects are not included.

An alternative calculation uses `SP_from_C(C,20,0)` before conversion back to EC_{25}. It changes the class of X08 from oligohaline to mesohaline, V02 from mesohaline to polyhaline, V06 from euhaline to hyperhaline and V07 from polyhaline to euhaline. This is a systematic reference-setting scenario, not a second measurement. The X03 tap value is retained exactly as submitted, $0.0954\,\mathrm{mS\,cm^{-1}}$.

Density-aware mixing scenario

Practical Salinity is not a conserved mass concentration. Within an imposed reference-seawater composition, Reference Salinity is proportional to Practical Salinity, so the component mass balance can be expressed in the latter units. To examine the approximation in volume-weighted seawater equivalents, this idealised scenario solves

$$\rho(s_r, T)(s_r - s_m) = r\rho(s_t, T)(s_m - s_t), \tag{7}$$

where s_m and s_t are the mixture and tap equivalents, s_r is the unknown source equivalent and r is the precisely measured tap-to-river volume ratio. Density is evaluated with `gsw.rho_t_exact`, setting Absolute Salinity equal to Reference Salinity from `gsw.SR_from_SP`, at zero sea pressure [19, 31, 32]. This imposes reference-seawater composition on both waters. It is an explicit scenario, not validation of the actual river or tap chemistry. It uses component masses from the original volumes without assuming additive final mixture volume.

The principal density calculation assumes a common component preparation temperature equal to the recorded mixture temperature; component temperatures when the volumes were measured were not separately recorded. Common 20 and 25 °C alternatives have little effect on the results below. The separate 20 versus 25 °C conductivity-reference scenario remains as described above. Precisely measured volume ratios are unchanged.

Table 6: Idealised density sensitivity at the working 25 °C conductivity reference. Values are $\mathrm{mS\,cm^{-1}}$ EC_{25} equivalents. Endpoints still cover only the meter allowance within the selected conversion model.

	Chet Mouth X01	Reedham V09	Oulton X07
Working central	34.821	32.198	8.030
Density central	34.499	31.925	8.030
Density lower endpoint	33.915	31.338	7.820
Summer scenario maximum	33.490	29.734	Not fitted
Remaining margin	0.425	1.604	Not applicable

The Chet lower-endpoint margin falls by approximately 42% and Reedham's by 14%, but both remain positive in this particular scenario. No descriptive salinity class changes. Oulton is undiluted, so density weighting has no effect. If its display instead represented EC20, its equivalent EC_{25} lower endpoint would be 8.686, still above the native historical maximum of 6.781. These checks do not establish robustness to unmeasured ionic composition, calibration bias or comparator error. The 216-row scenario output and executable calculation are supplied.

For historical EC20, the nominal bridge is $G_{25}[F_{20}(C_{20})]$. It assumes seawater-equivalent composition and is not an empirical calibration across all natural waters. A same-source-sample pair at Buckenham on 3 March 2020 contains 650 and 718 $\mu\mathrm{S\,cm^{-1}}$ at 20 and 25 °C. The GSW bridge predicts 722.94, approximately 0.69% above the paired EC25 result. One freshwater pair cannot validate the bridge at higher salinities. Native EC20 and EC25 populations therefore remain separate, with the nominal bridge and its ±10% perturbations treated as sensitivity tracks.

The conventional fresh, oligohaline, mesohaline, polyhaline, euhaline and hyperhaline bands are applied as descriptive seawater-equivalent intervals. Figure 6 shows every observation and its instrument endpoints. No class changes under those endpoints. This consistency does not remove the systematic reference-setting uncertainty or identify biological impact thresholds.

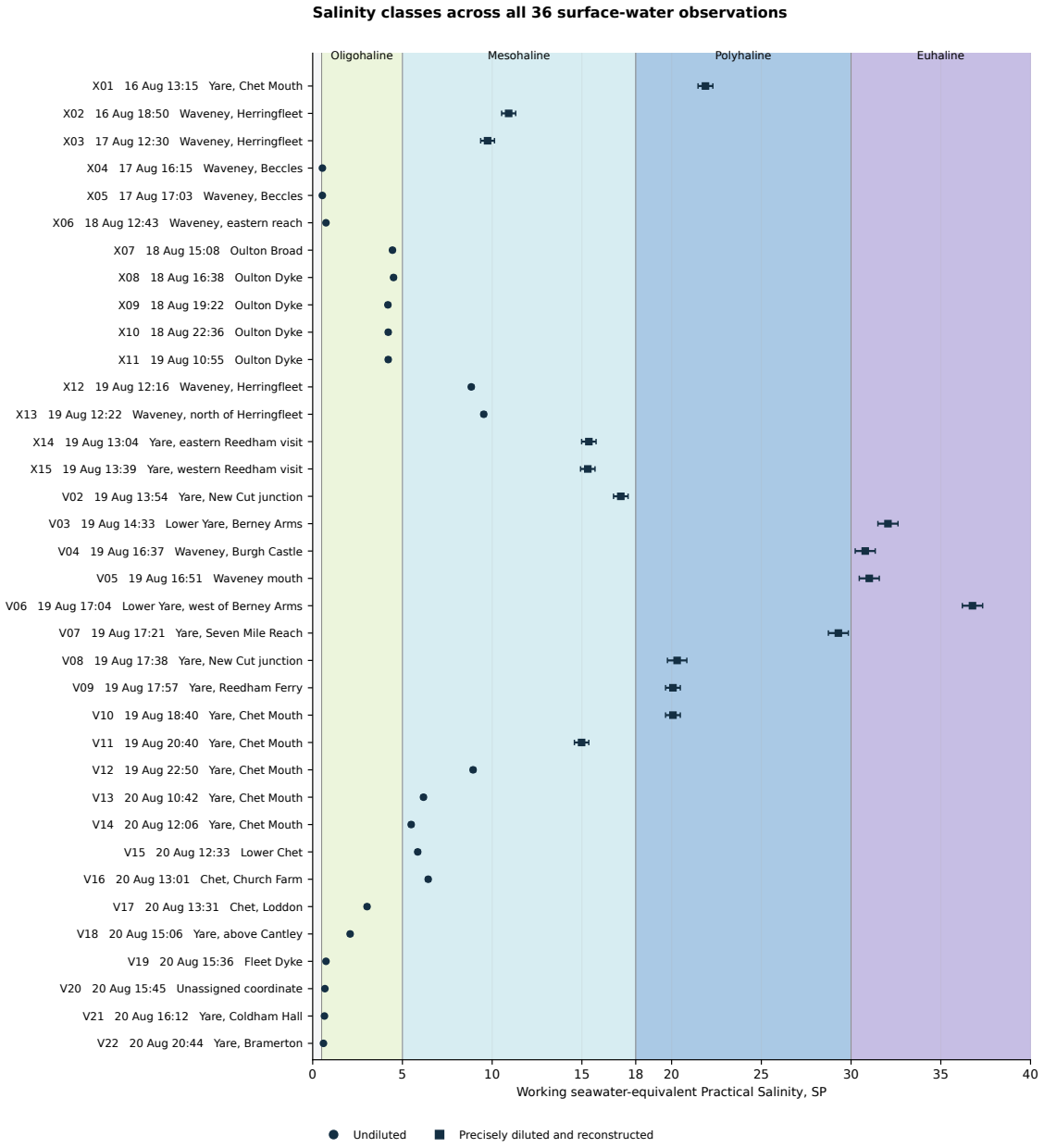


Figure 6: All 36 observations on the seawater-equivalent salinity scale. The classification describes the field value, not its rarity. Instrument endpoint bars omit calibration, composition and reference-setting uncertainty.

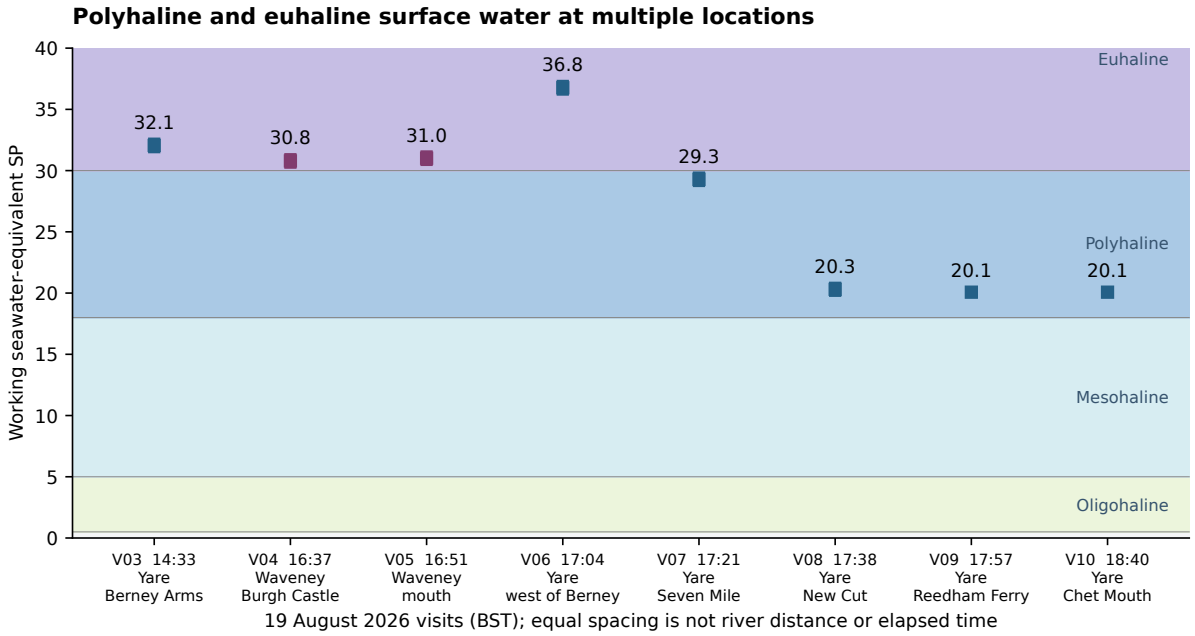


Figure 7: Eight observations during the high-salinity part of the 19 August route. All eight are dilution-derived. Agreement across locations supports the spatial pattern but cannot exclude a shared systematic conversion effect. Visit ordering is not a simultaneous longitudinal profile.

C Historical chemistry and descriptive distributions

The complete five-station source pull contains 21,486 observations across all determinands. Its 923 salinity observations comprise 916 direct in-situ measurements and seven legacy chloride-derived results. Text matches to unionised ammonia in saline water are not salinity. Analytical inclusion further requires appropriate water material, an exact numeric result, eligible source flags and a date before 2026. These distinctions explain why the primary direct-salinity cohort is smaller than the full archive.

Four zero results from a single sampling run on 15 July 2021 are excluded as suspect in the primary distributions and retained in source audit records. This is a quality judgement, not proof that every zero in tidal waters is invalid. Censored chloride-derived results, such as values below a detection limit, are not placed in ordinary histograms as exact values. Native EC20 and EC25 remain separate, as do water-column and sediment/interstitial materials.

Table 7: Primary pre-2026 direct-salinity archive. JAS denotes July to September. Station-days have equal descriptive weight.

Station	Location	Days	Years	JAS	August
AN-WAV179	Burgh Castle	186	19	48	15
AN-YAR2625	Berney Arms	175	19	45	14
AN-BWY004P	Breydon main channel	168	18	43	13
AN-YAR268	Cobham Island	160	18	41	13
AN-YAR270	Haven Bridge	138	16	35	10

The native Oulton Broad EC_{25} population has 46 lake-water station-days and an all-year median of 1.560, P90 of 3.415 and maximum of 6.781 $\mathrm{mS\,cm^{-1}}$. The native summer non-drought population has nine dates, median 2.400 and P90 2.842. Two drought dates are reported as individual observations rather than a reliable tail distribution. Its record covers only five sampled calendar years. A Loddon value of 51,100 $\mu\mathrm{S\,cm^{-1}}$ on 10 September 2001 (source sample 1151239) is excluded as discordant with same-sample chloride of 67 $\mathrm{mg\,L^{-1}}$; no corrected value is invented. A low Bramerton value of 67 $\mu\mathrm{S\,cm^{-1}}$ on 11 September 2007 (sample 1473915) remains a separate sensitivity. The St Olaves native EC25 record has 35 station-days in 2000 to 2002; its all-month maximum is 19.1. Its separate 47-day EC20 record in 2003 to 2006 supplies the higher summer comparator for Herringfleet. Missing years and changes in measurement method are not interpreted as environmental trends.

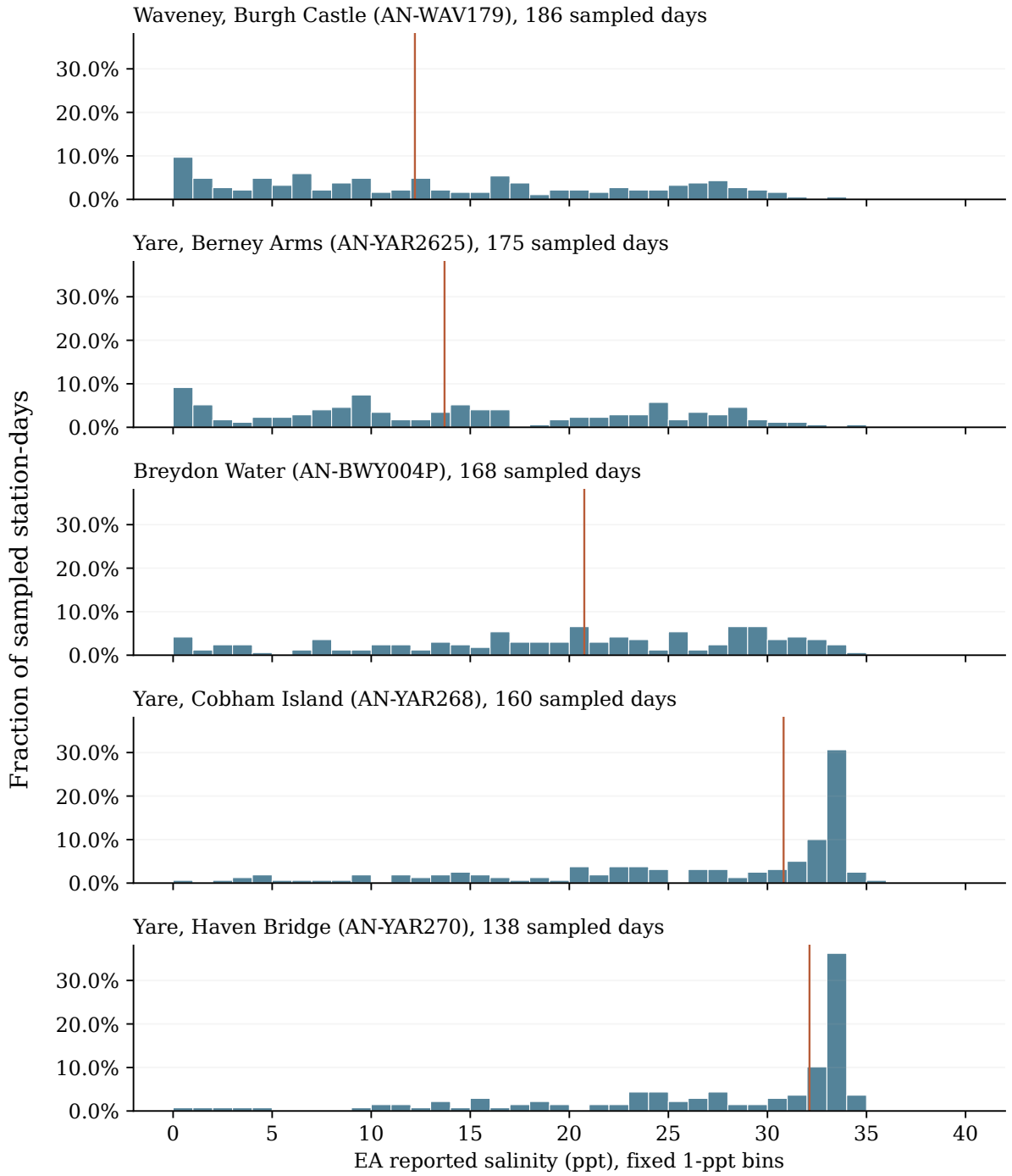


Figure 8: Historical direct-salinity distributions at the five substantial estuarine stations. Bars describe sampled station-days, with equal weight per day and fixed bins. Orange lines mark medians. They are not time-occupancy probabilities and do not remove seasonal or tidal sampling imbalance. The companion tables distinguish all-year, summer and August populations.

D Flow reconstruction and tidal evidence

D.1 Gauged contributions and their interpretation

The flow analysis uses five NRFA gauges, extended by EA daily records [11, 33]. Historical source values retain priority within their period of coverage. Eligible numerical zero flows are retained; missing, suspect, negative and incomplete values are excluded. Estimated historical values and unchecked recent values retain their source flags. The source table contains 116,072 gauge-date rows, including explicit calendar gaps, of which 114,074 meet these rules. These counts are not counts of independent hydrological events.

Table 8: Gauged contributions used to describe freshwater supply. Areas are metadata for the gauged catchments, not weights used to extrapolate total river discharge.

NRFA	River and gauge	Area (km^2)	Main source qualification
34001	Yare at Colney	231.8	Groundwater augmentation and seasonal abstraction
34002	Tas at Shotesham	146.5	Groundwater abstraction and effluent returns
34004	Wensum at Costessey Mill	570.9	Low-flow abstraction, estimated historical values and a July 2006 qualification
34006	Waveney at Needham Mill	370.0	Summer groundwater support and a revised rating
34019	Bure at Horstead Mill	313.0	Gate operation and historical reprocessing

The Yare index is the sum of Colney, Shotesham and Costessey. The regional index additionally includes Needham and Horstead. All component gauges must be eligible for a composite daily value. Directed paths in the mapped surface-river network connect each gauge to a distinct downstream confluence and show that none lies on another gauge's downstream path. This supports aggregation without double-counting nested main-river gauges. It does not establish independence of groundwater, artificial transfers or downstream exchange.

The contributing gauged areas total 949.2 km^2 for the Yare index and 1,632.2 km^2 for the regional index. No drainage-area scaling is applied to estimate ungauged flow. These indices describe realised, artificially influenced gauged supply. They omit downstream inputs, travel-time differences and ungauged drainage, so they are not total freshwater discharge at a boat location.

Daily source periods follow the water-day convention beginning at 09:00 GMT. For a visit on date d, the most recent included source date is $d - 2$. This conservative join avoids using any part of an unfinished source period when chemistry clock conventions are uncertain. Every Q_7 and Q_{28} value requires complete eligible component days. This reporting offset is not an estimated estuarine transport lag.

The seasonal drought threshold uses at least 24 represented years and 80% of the possible values in each 1991 to 2020 reference window. Estimated observations contribute to approximately one-fifth of eligible Yare and regional reference windows. Excluding all estimates makes those composite seasonal thresholds unavailable under the fixed completeness criterion. The criterion is not relaxed to manufacture a replacement result.

During the five survey dates, the Yare Q_7/P20 ratio rises from 0.574 to 0.666 and the regional ratio from 0.709 to 0.762, both within classified drought episodes. Needham ranges from 1.629 to 1.661 and is classified non-drought. Regional drought and tributary-specific realised flow therefore convey different information. Needham is also an upstream proxy rather than a measurement of Oulton Broad's exchange or flushing rate.

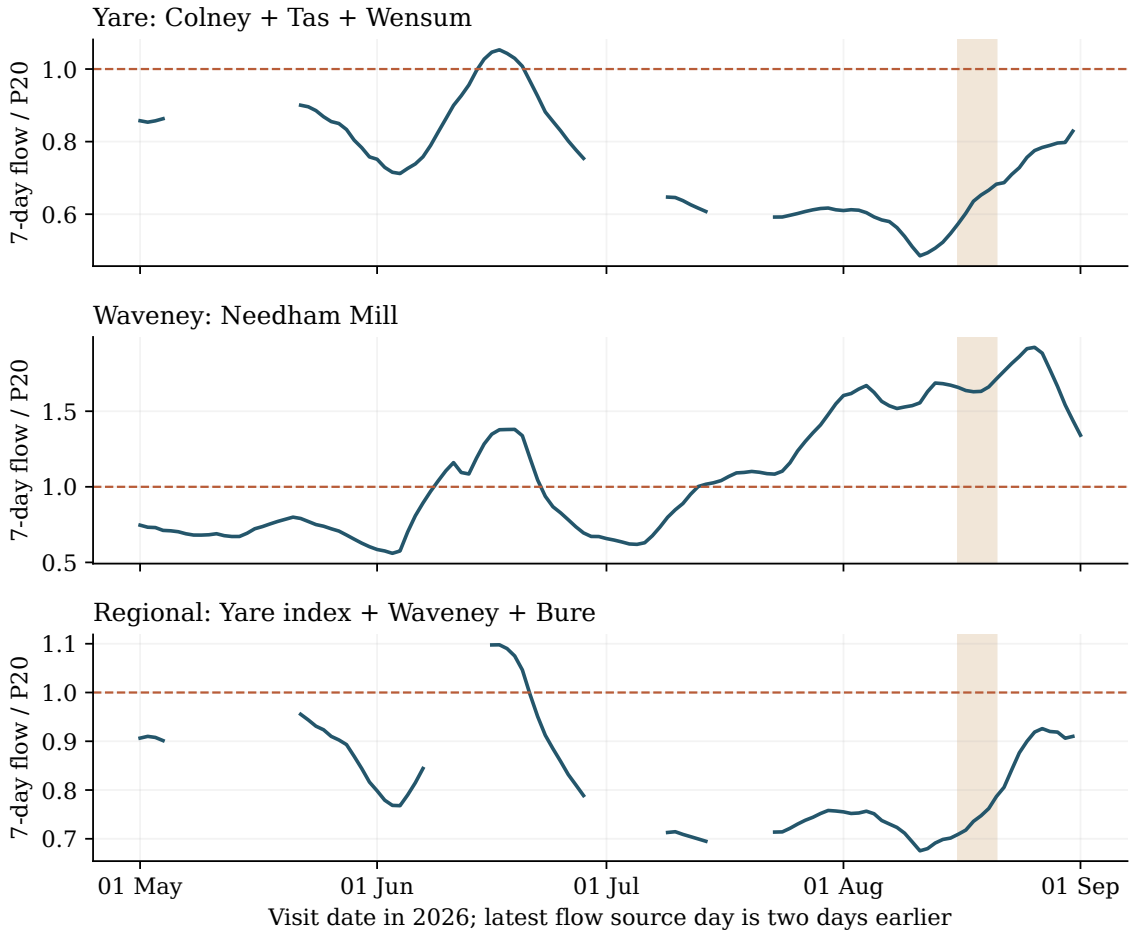


Figure 9: Gauged flow relative to its seasonal P20 threshold. Shading marks 16 to 20 August. Drought additionally requires a low-flow run lasting at least 14 valid days. Flow source dates are shifted forward by two days to show the visit-date convention. Gaps remain where source values are missing or excluded. This descriptive plot retains the source daily classification; the separate Tas reconstruction below supplies antecedent-state sensitivities. Recent EA values are provisional.

D.2 Antecedent-flow recovery

Five Tas days with incomplete daily summaries have 96 numerical subdaily observations, all flagged Good. Averages over the complete water-day recover those days without modelling an unobserved flow. Against 24 complete official daily means, independently calculated means agree within $0.000479\,m^3\,s^{-1}$, consistent with the official rounding precision.

Four consecutive quarter-hour observations on 14 July remain unavailable. Interpolation between measured neighbouring values supplies a central reconstructed daily mean of $0.119979\,m^3\,s^{-1}$. An independent masking experiment uses 116 one-hour blocks across 29 other pre-August days. Point MAE is $0.000664\,m^3\,s^{-1}$ and block-mean MAE is $0.000547\,m^3\,s^{-1}$. Perfectly correlated within-hour error scenarios produce daily means from 0.119688 to $0.120052\,m^3\,s^{-1}$. The blocks are temporally related, so their number does not imply 116 independent hydrological episodes.

The reconstructed hour remains labelled estimated. These scenarios improve antecedent-state availability without changing the field-date Q_7 or Q_{28} values. A source-only alternative leaves the hour unresolved and applies a substantially wider driver-range sensitivity. Neither the empirical interpolation-error range nor that wider scenario is a guaranteed probabilistic bound.

D.3 What historical tide information establishes

The direct-salinity archive contains 873 eligible pre-2026 observations on 827 station-days. Complete antecedent-flow features retain 697 observations; a complete depth field retains 661. The matched flow, depth and tide-clock cohort has 495 observations on 480 station-days in 14 years. These are successive eligibility restrictions, not conflicting estimates of one sample size.

The recorded high-water variable is an HH.MM clock: for example, 10.5 represents 10:50. All 649 strings parse. The same clock is shared among sampled stations on 121 of 130 dates, indicating a common trip or reference-port clock rather than independently measured local high water. Fourteen observations on three inconsistent dates are excluded from this proxy before the other feature restrictions. Its reference port, timezone and observed-versus-predicted status are not established.

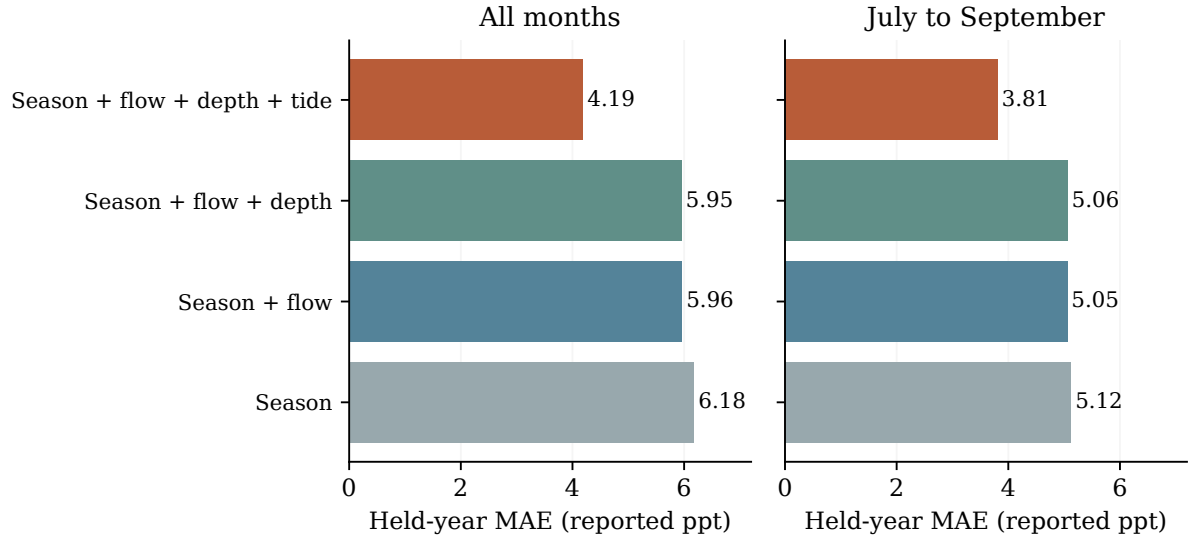


Figure 10: Historical predictive value of a recorded tidal-clock proxy. Exactly the same 495 observations are used in all four models. Errors are averaged equally across the five stations after whole-year holdout. Adding the tide clock reduces all-month mean absolute error by 29.6%. Its unresolved reference prevents direct deployment at boat times. This diagnostic is separate from the M2 and observed coastal features used in the actual-coordinate models.

Observed water-level context is supplied separately by 2,304 quarter-hour readings at six gauges over 18 to 21 August. Gauge datums remain distinct. Reedham low water occurs at approximately 23:00 BST on 19 August and 10:45 BST on 20 August; the 22:50 and 10:42 samples are consequently close to nearby-gauge low water. At 12:06 the gauge level is rising. These timings describe nearby water levels, not measured current direction, the exact time of a salinity maximum or whole-channel flushing.

D.4 Coastal features and reconstruction validation

Historical Lowestoft levels are drawn from GESLA/BODC with their source quality flags [6, 16, 35]. The 2026 EA Lowestoft extension contains 8,700 of 8,832 expected quarter-hour values from June to August, or 98.51%. Recent records are provisional. Because the historical datum is unspecified while the recent series is in metres AOD, only quantities invariant to an additive datum shift are transferred.

The coastal anomaly is the mean level during the preceding 72 hours minus the mean over the preceding 30 days ending 72 hours earlier. The range is the maximum minus minimum over the preceding 25 hours. Source-based features require at least 95% of expected observations over fully elapsed windows. This distinguishes the recent anomaly from a mean that overlaps its reference window.

Historical gaps are reconstructed retrospectively using source-good Cromer and Felixstowe levels, local harmonic terms and a linear trend. Each fit excludes the target gap and uses 90 days on either side. Neighbour predictors use current, two-hour-lagged and four-hour-lagged levels plus a preceding 25-hour mean. Eight fixed periods, in hours, are 12.4206012, 12, 12.6583475, 23.9344721, 25.8193387, 26.8683567, 6.2103006 and 6.1033393. Standardised ridge penalisation is 1. Predictions are averaged when both neighbouring gauges are available. A harmonic prediction with a slowly varying residual bridge supplies fallback where both are unavailable. This method uses observations after the historical gap and is therefore a retrospective reconstruction, not an operational forecast.

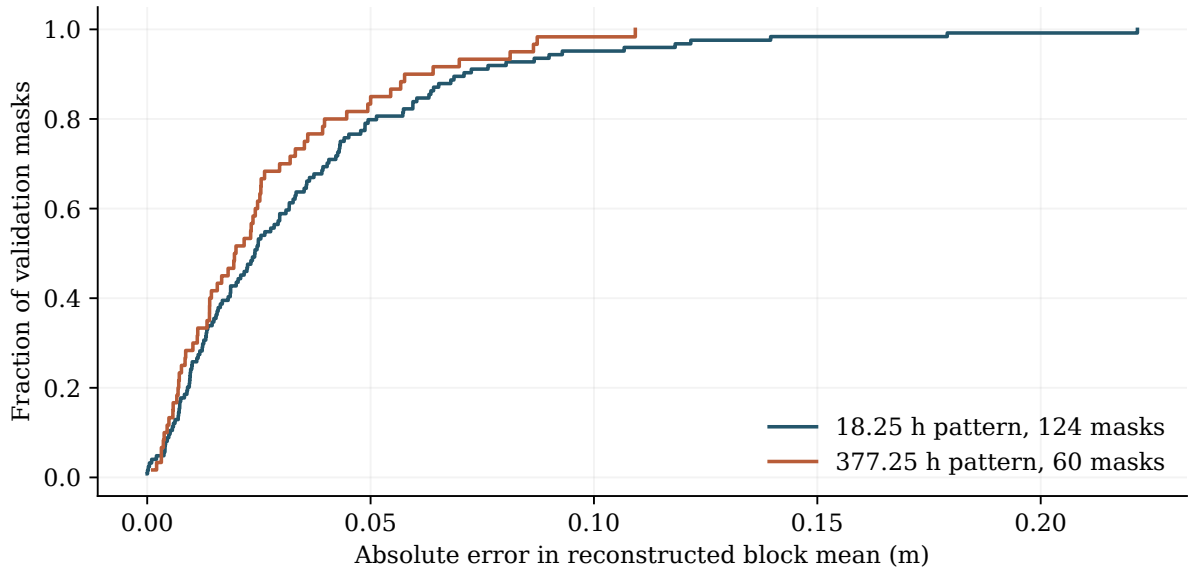


Figure 11: Withheld-block coastal reconstruction errors for the actual 2009 and 2010 missingness patterns. The 377.25-hour pattern includes periods without measured neighbouring-gauge support. Curves describe fractions of validation masks, not independent drought events or a guaranteed uncertainty distribution. Whole-block error trajectories are shared across chemistry observations affected by the same historical gap.

The 377.25-hour pattern has 60 masked tests with mean level MAE 0.0974 m and a 95th percentile absolute block-mean error of 0.0815 m. The 18.25-hour pattern has 124 tests with corresponding values 0.0754 and 0.0925 m. Additional generic-duration tests total 563 masks; some overlap and are not independent. Reconstruction permits retention of 20 Chet and ten Reedham chemistry dates whose forcing windows would otherwise fail completeness, including high-conductivity dates. One hundred shared-block error trajectories propagate reconstruction uncertainty. Source-good covariates remain unchanged and reconstructed values are never relabelled measured.

E Regression specifications and predictive validation

E.1 Lower-Yare design and sensitivity family

The conductivity training sites are Haven Bridge, Reedham Ferry, Chet Mouth and Cantley Red House. Their response methods and water-material labels remain explicit. The reconstructed-forcing cohort contains 252 native EC25 and 174 native EC20 observations. The five method tracks are native EC25, native EC20, a nominal bridge and two bridge perturbations of ±10%. Two clocks, two spatial bases, two coastal specifications and two response transformations give 80 variants. Sixteen native-EC20-only variants are not compared numerically with field EC25, leaving 64 field-comparable variants. The displayed coastal calendar family contains 32 variants. These are related model specifications, not independent confirmations.

Let river chainage r be kilometres upstream from Berney and set $x = (r - 5)/10$. Define dimensionless flow predictors

$$q = \log(1 + Q_7/Q_0), \qquad a = \log(1 + Q_{28}/Q_0) - q, \qquad Q_0 = 1\,\mathrm{m^3\,s^{-1}}. \tag{8}$$

The annual phase is $A = 2\pi(\mathrm{DOY} - 1)/365.2425$. M2 phase M advances at 28.9841042 degrees per hour from 1 January 2000 UTC. The full coastal quadratic predictor is

$$\begin{aligned}\eta = {} & \beta_0 + \beta_x x + \beta_{x2} x^2 + \beta_{As} \sin A + \beta_{Ac} \cos A \\ & + (\beta_q + \beta_{xq} x) q + (\beta_a + \beta_{xa} x) a \\ & + (\beta_{Ms} + \beta_{xMs} x) \sin M + (\beta_{Mc} + \beta_{xMc} x) \cos M \\ & + (\beta_H + \beta_{xH} x) H + (\beta_R + \beta_{xR} x) R.\end{aligned} \tag{9}$$

The radial-basis alternative replaces x^2 by two Gaussian terms centred at $r = 0$ and 10 km with 10 km width. The quadratic form has 12 non-intercept predictors without coast and 16 with coast; the radial form has one more. The response is numerical C/C_0 or $\log(1 + C/C_0)$, where $C_0 = 1\,\mathrm{mS\,cm^{-1}}$. Nonnegative inverse prediction is applied after residual addition when estimating predictive quantiles. The inverse fitted centre alone is not necessarily a predictive mean or median.

Standardised ridge penalisation is fixed at 10. Sine/cosine pairs share a root-mean-square scale so the penalty does not prefer an arbitrary harmonic origin. Fit weights give equal total weight to stations and then to years within station. No 2026 field response enters coefficients or residual calibration. The investigation nevertheless began after the field values were known and is not a preregistered prospective test.

E.2 Spatial and temporal validation

Whole-year holdouts respect temporal dependence [28]. A strict spatial route additionally removes the entire target station from fitting and residual calibration. An inner site/year holdout generates calibration errors without the outer site or year. The nearby-station route instead transfers known-station held-year errors to a boat coordinate under a local-smoothness assumption. Good performance in the broader strict route does not validate the narrower local route.

Table 9: Selected July to September nested validation results for the British-clock quadratic coastal log model. MAE is in mS cm^{-1}. Coverage describes these finite historical tests, not guaranteed coverage under the 2026 forcing.

Validation route	Response track	n	MAE	Upper coverage
Strict spatial, interior sites	Native EC25	23	3.691	23/23
Strict spatial, interior sites	Nominal bridge	46	3.116	46/46
Local Reedham	Native EC25	6	3.607	5/6
Local Chet Mouth	Native EC25	17	3.596	15/17
Local Reedham	Nominal bridge	18	3.482	16/18
Local Chet Mouth	Nominal bridge	28	2.747	25/28

The native strict summer set spans seven years. Corresponding radial-basis coverage is 0.739 for native EC25 and 0.848 for the nominal bridge, despite similar central errors. Those variants remain exploratory sensitivities rather than calibrated 95% procedures. Native lower-model training includes no summer drought responses. The nominal bridge adds 11 pooled summer drought observations, including three at Reedham and two at Chet Mouth from one local episode each.

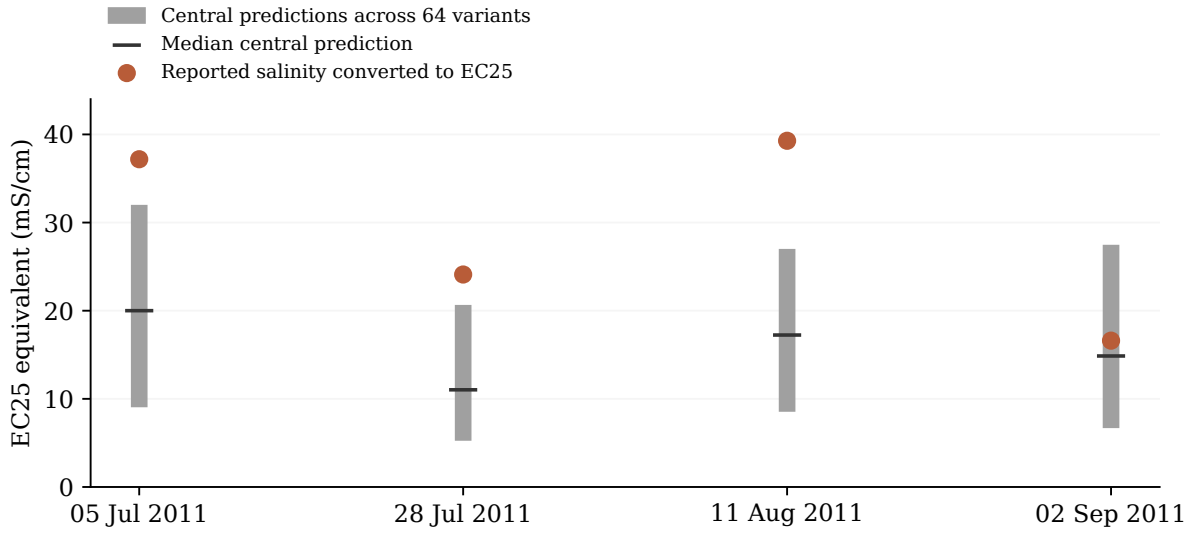


Figure 12: External shallow-water check at Berney. Four direct-salinity observations at reported 0.2 m depth are converted to EC25 only for this diagnostic. Grey ranges show central predictions across 64 model variants, not predictive intervals. All variants underpredict on average. This evidence prevents use of the conductivity surface as an authoritative central baseline in that lower reach.

The four Berney equivalents are approximately 37.19, 24.11, 39.28 and 16.60 mS cm^{-1}, compared with reference predictions of 10.77, 5.25, 10.33 and 9.43. Mean underprediction is 20.35 mS cm^{-1}. The diagnostic is cross-method and small, but sufficiently adverse to reject that low central curve as an authoritative local expectation. The separate direct-salinity station archive remains the comparator.

E.3 Upper-river and direct-estuary models

Upper-Yare fits use Bramerton, Coldham and Buckenham. The full cohorts contain 579 native EC25 and 134 native EC20 observations; coastal completeness retains 200 and 124. Native EC20 remains a separate track here. The unweighted standardised ridge model has penalty

10, $x = (r - 22.2035448682)/10$ and 11 base terms: chainage, q, a, annual and M2 sine/cosine terms and chainage interactions with q, a and M2. Coastal variants add H, R and xH. Raw/log responses and both clocks remain separate. Residuals are equally weighted by year within comparator.

For the full-record native-EC25 British-clock log/year model, residual-corrected median MAE is $0.0606\,\mathrm{mS\,cm^{-1}}$ at Bramerton, 0.0552 at Coldham and 0.0572 at Buckenham. Summer upper coverage is 50/51, 45/47 and 47/50, respectively. These median errors are not the same statistic as central-prediction errors in Table 9. Coldham's 47 summer tests span 17 years but include only two native summer drought observations. Three-observation EC20 drought holdouts represent one episode and give much less stable coverage.

The above-Cantley scenario uses 457 native EC25 observations over 21 years and 16 configurations. Its main residual mixture assigns 0.586812 weight to Cantley and 0.413188 to Buckenham by river distance. Endpoint-only transfer tests that unverified spatial assumption. Same-date triples cannot establish an instantaneous gradient: the 16 complete-flow summer triples can span 6.93 hours. Loddon's legacy marina model has 74 training observations and 16 summer residuals in seven years, but no summer drought training response.

The separate direct-estuary models retain EA-reported ppt rather than conductivity. Summer validation at Berney has 29 observations, MAE 5.029 reported ppt and nominal 90% envelope coverage 27/29. Burgh Castle has 29 observations, MAE 5.320 and coverage 25/29. These are known-station diagnostics. They do not validate a timed prediction at a geographically separate boat position.

E.4 Historical scenario populations and support

The lower coastal calendar covers July to September 2000 to 2011: 836 non-drought days and 67 drought days in three episodes. All 24 UTC hours are evaluated with their paired flow and coastal history. The 2006 episode contributes 46 of the 67 drought days; equal-episode weighting checks that dominance. The full upper-river calendar has 1,838 non-drought days and 214 drought days in nine episodes during 2000 to 2025. Its shorter coastal subset contains 707 non-drought and 55 drought days in three episodes, including some partly observed days that are date-weighted.

These are model evaluation populations, not salinity training observations. About 79.1% of native lower drought-calendar states lie below at least one training-flow minimum and about 91% lie outside the joint log-flow convex hull. The bridge reduces the marginal below-range fraction to 38.8%. The strict historical joint Q_7/Q_{28} severity match to the 19 and 20 August field forcing contains no drought day; a 5% tolerance admits eight days in one 2006 episode. These support checks concern those specified forcing states and are not a declaration that no historical Broads drought was comparable in every respect.

The residual distribution in Equation 3 is transported across normal and drought states. A separately drought-dependent residual variance or tail is not identified. More hourly evaluations improve numerical representation of the chosen calendar but do not add independent drought evidence. A finite mixture CDF reaching one must not be reported as zero probability of a future exceedance.

E.5 Response-memory experiment

The dynamic experiment uses the same 252 native EC25 observations for 16 combinations of two clocks, two response transformations and four response times. Only q, a, H and R are filtered. Annual and M2 terms remain outside the state. No August salinity is used for initialisation. Initial-state sensitivities are ± 100 raw conductivity units or $\pm \log(101)$ latent units, with exponential decay. Missing driver intervals use past-only holding and export the residual missing-data weight. These are declared sensitivity scenarios, not physical maxima.

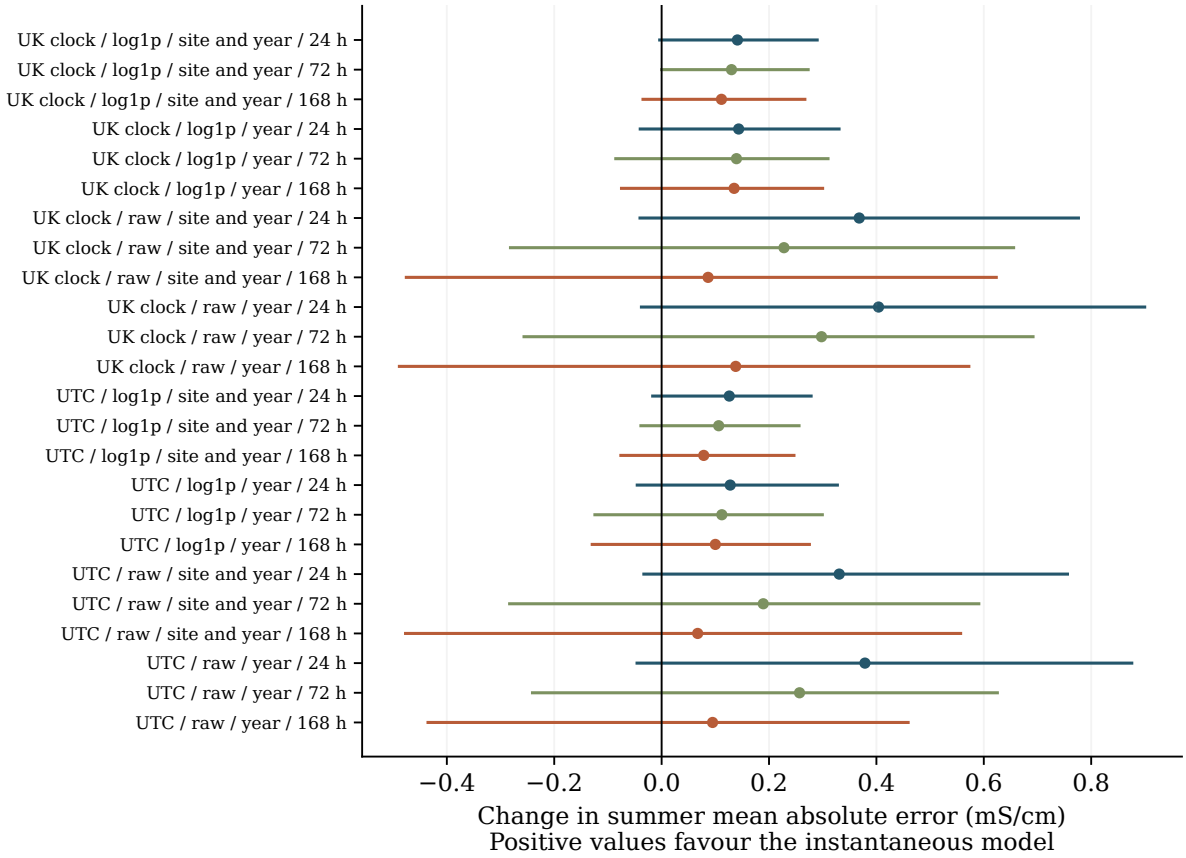


Figure 13: Response memory versus instantaneous forcing. All 24 changes in summer mean absolute error are positive, favouring the instantaneous benchmark. Lines show empirical year-block 95% intervals; 23 include zero. The comparison covers clocks, response scales, validation routes and response times. It does not independently validate dynamic predictive-tail coverage.

The sparse historical grabs do not identify a superior response-memory scale. Dynamic upper comparisons therefore remain sensitivity calculations based on transferred historical residuals. Historical coastal reconstruction errors are propagated jointly in the static analysis, not through every dynamic state. A source-only flow alternative and all-season maximum-error stresses remain broader tests rather than interchangeable versions of a nominal summer P95.

F BFI benchmark and alternative models

F.1 Published occurrence model

BFI Product 25d, HR Wallingford report DER7003-RT001 R07-00 dated 14 March 2025, models threshold occurrence during whole tidal cycles and high and low conductivity within identified events [18]. It describes 101 occurrence and 96 intensity configurations. Cantley and Rockland Broad are relevant southern-system fixed gauges. Event-cycle probabilities are not point-time salinity predictions at boat coordinates.

For Cantley with Colney flow and Great Yarmouth water levels, the printed August coefficients for a $3.4\,\mathrm{mS\,cm^{-1}}$ threshold give

$$\operatorname{logit} P = -6.38 + 5.20HW + 2.14LW_{\text{previous}} - 2.70FL. \tag{10}$$

Tidal levels must be metres AOD and FL is flow in $\mathrm{m^3\,s^{-1}}$. The required preceding 24-hour flow is approximated here by the latest complete daily water-day. The source datum was checked before applying the coefficients.

Table 10: Independent evaluation of the published Cantley equation for two afternoon tidal cycles. The final column maximises the fixed equation over nonnegative freshwater flow; it is not a confidence bound.

High water, BST	HW	Previous LW	Daily FL	P	P at $FL = 0$
19 August, 14:00	1.123	−0.371	0.139	15.32%	20.84%
20 August, 15:00	0.960	−0.292	0.164	7.90%	11.79%

Overlap-weighted adjacent daily means give afternoon probabilities of 15.18% and 7.84%, but cannot represent every possible within-day flow profile. Equation 10 supplies an independently published gauge-level benchmark, not a p-value for a boat sample. Coefficient uncertainty and predictive model error are absent from the zero-flow calculation. Independently fitted higher-threshold regressions cross at very small probabilities, so they cannot simply be inverted into a monotone salinity distribution.

F.2 Intensity-model limits

The published intensity equations require previous-cycle high and low conductivity and predict event extrema. The field survey does not supply those preceding gauge states. The report gives Cantley occurrence AUC 0.936 and intensity high-conductivity $R^2 = 0.71$, RMSE $4.004\,\mathrm{mS\,cm^{-1}}$, with low-conductivity $R^2 = 0.78$, RMSE $1.975\,\mathrm{mS\,cm^{-1}}$. Independent year/event holdout and predictive-tail coverage are not documented. AUC and RMSE do not determine a conditional upper percentile.

There is a printed transformation ambiguity. Page 46 defines, in source units of $\mu\mathrm{S\,cm^{-1}}$,

$$z = \log\{(52000 - C)/C\}, \tag{11}$$

whereas page 47 prints $C = 52000\exp(z)/(1 + \exp(z))$ as its inverse. Composing the two returns $52000 - C$. The inverse of the printed forward transformation is instead $52000/(1 + \exp(z))$. An

increasing-logit forward transformation would match the printed increasing inverse. The fitted implementation is needed to establish which convention produced the coefficients. No convention is silently repaired here and 52 mS cm^{-1} is not treated as a physical salinity bound.

Candidate trajectories under an explicitly increasing-logit convention were examined over 28 ordered initial-state pairs and ordinary or zero-flow scenarios. Their finite ranges are deterministic state sensitivities, not probabilistic limits. They exclude residual model error and do not cover arbitrary initial states approaching the imposed cap. The report's spatial interpolation exercise is also described as inconclusive. These restrictions concern transfer to this study's estimand, rather than invalidating the report's gauge-level work.

F.3 Other model choices

A calibrated salt-transport model could represent channel geometry, boundary salinity, freshwater inflow and branch exchange directly. Such a model would also need bathymetry, mixing parameters and time-resolved calibration. No deterministic advection-dispersion or hydrodynamic salt-balance model is fitted here. Chainage regression and forcing-memory regression should not be described as such models.

Kang et al. [20] combine empirical mode decomposition and random forests for a continuous daily estuarine record. That approach is a relevant option where sufficiently long response series exist. The reported design decomposes the complete series before random training/test splitting; blocked or prospective validation would be needed before interpreting that performance as independent future-period prediction. The present sparse, method-changing grab archive does not provide equivalent time-series support. No random-forest model is fitted or directly benchmarked in this study. Greater flexibility would not itself supply missing severe-drought episodes, identify branch exchange or remove unobserved spatial transfer.

G Spatial extent calculation

Frozen OpenStreetMap waterway extracts define approximate channel centrelines [25]. Ways are merged by identifier and projected to a local metre grid at 52.55 degrees north. Each observation is projected to the nearest eligible named channel. For a specified date and salinity threshold, the maximum shortest-path distance between qualifying projected points defines the endpoint span within that channel. Named channels are treated separately and their non-overlapping lengths are summed. No unsampled route through New Cut or across an open broad is inserted.

The principal same-day spans are 8.979 km on the Yare, from V03 to V10, and 9.826 km on the Waveney, from X12 to V05. All threshold-qualified points are within 38.3 m of mapped centrelines. Tightening the geometric admission cutoff from 100 to 50 m leaves the 18.805 km and 21.757 km results unchanged. The full-period Chet contribution is 2.952 km. The polyhaline-or-higher sum consists of 8.979 km on the Yare and 1.459 km on the Waveney.

The broader named-channel survey spans are 27.825 km on the Yare, 22.795 km on the Waveney and 4.665 km on the Chet. They total 55.284 km under the stated projection rule. The Beccles coordinate is approximately 156 m from the frozen centreline, Oulton Broad lacks a suitable open-water centreline and V20 is not assigned to a verified channel. These locations remain in the field tables and map but do not extend this length measure. Single-coordinate branches contribute zero additional span. Values are rounded in prose because map geometry limits accuracy.

The 18.8 km result concerns the distances between selected same-day observations. It does not assign concentrations to intervening points, prove that conditions were simultaneous or identify the length historically anomalous under drought. The Broads Authority's more-than-200 km navigation figure also includes broads, so the comparison is contextual rather than a like-for-like estimate of affected habitat area or network percentage.

H Answers for all location groups

The following table retains all 24 location groups. Q1 and Q2 distinguish normal and drought historical expectations; Q3 states what the visits show against those expectations. Values are working EC_{25} in $mS\,cm^{-1}$ except where the EA salinity-model scale is explicitly stated. "No baseline" means that no defensible exact-location distribution was established, not that the field value is normal. A transferred comparator and an exact-location prediction have different evidential scope.

Table 11: Answers at each of the 24 sampled location groups. All values are conductivity normalised to 25 °C, in mS/cm, except five lower-estuary rows explicitly labelled as SP equivalents versus EA-reported ppt. M is the median and P90 the 90th percentile. "Normal" means historical July to September non-drought conditions under the catchment flow rule; "drought" uses the corresponding historical drought subset. Ranges span retained model variants or closely spaced visits, not confidence intervals. Proxy values describe the named comparison reach, not a validated local distribution. Nominal actual-time P95 and sensitivity maxima answer a different question from a seasonal P90; maxima across tested scenarios are not calibrated 95% prediction limits.

Location and field observations	**Q1: Normal conditions**	**Q2: Drought conditions**	**Q3: Comparison and limits**
Yare at Chet Mouth X01, V10, V11, V12, V13, V14 EC25 9.77 to 34.82	M 1.67 to 3.47; P90 8.28 to 12.43. Nearby confluence model.	M 2.21 to 6.05; P90 10.36 to 15.01. Historical summer drought calendar.	X01: field lower limit 34.225 exceeds nominal actual-time P95 29.127 and summer sensitivity maximum 33.490. Broader Tas-flow extreme 41.295 accommodates it. V10: central 32.198 exceeds nominal 30.693, but lower limit 31.601 overlaps sensitivity maximum 31.926. V11 to V14 lie within conditional bounds. Transfer is qualified, not exact-site validation.
Waveney at Herringfleet X02, X03, X12 EC25 15.19 to 18.46	St Olaves proxy: M 1.670; P90 2.872, 9 summer non-drought EC25 dates.	St Olaves legacy EC20: two summer drought dates, nominal EC25 equivalents 4.656 and 8.076. No reliable drought-tail estimate.	Field 15.190 to 18.460 exceeds the short native-EC25 summer reference, but remains below the older EC20 summer P90 equivalent of 19.642. No exact-site conditional anomaly is established. Comparator is 1.38 km away in straight line; EC20 and EC25 series remain separate.
Waveney at Beccles Quay X04, X05 EC25 1.086 to 1.093	No defensible local summer distribution.	No defensible local drought distribution.	Both visits have low conductivity, 1.086 and 1.093. Numerical salinity equivalents near the freshwater boundary are sensitive to freshwater ion composition. Historical rarity is not identifiable from the available local evidence.
Waveney, eastern reach X06 EC25 1.478	Burgh St Peter proxy: M 1.819; P90 2.710, 10 non-drought summer river-water dates.	Burgh St Peter proxy: M 2.805; P90 4.685, 10 drought summer dates.	Field 1.478 is below this downstream comparator's drought P90. The comparator is 3.63 km away in straight line. This is reach context, not a validated baseline for the sampled coordinate (52.46223, 1.62943).
Oulton Broad X07 EC25 8.03	Nearby lake-water EC25: M 2.400; P90 2.842, 9 summer non-drought dates.	Only two summer drought dates: 4.022 and 6.781. A reliable drought P90 is not estimated.	Field 8.030 and instrument lower limit 7.820 exceed the all-month local archive maximum 6.781 (46 EC25 dates). Central excess is 18.4%. The station is 77 m away. This is a local observed-archive exceedance; sparse drought coverage and unmodelled exchange prevent an exact-time drought-tail probability.

Continued on the following page

Table 11 continued

Location and field observations	Q1: Normal conditions	Q2: Drought conditions	Q3: Comparison and limits
Oulton Dyke X08, X09, X10, X11 EC25 7.60 to 8.13	Oulton Broad proxy: M 2.400; P90 2.842. No validated Dyke distribution.	Oulton Broad proxy: two summer drought values, 4.022 and 6.781. No validated Dyke drought tail.	Four direct visits give 7.600 to 8.130 across 18 h 17 min. Every instrument lower limit exceeds the Broad archive maximum. The Broad station is 1.79 km away in straight line, so this supports persistent brackish water at the Dyke but not a proven exact-site historical exceedance.
Waveney north of Herringfleet X13 EC25 16.29	St Olaves proxy: M 1.670; P90 2.872, 9 summer non-drought EC25 dates.	St Olaves legacy EC20: two summer drought dates, nominal EC25 equivalents 4.656 and 8.076. No reliable drought tail.	Field 16.290 is above the short native-EC25 summer reference but below the older EC20 summer P90 equivalent 19.642. The station is 0.70 km away in straight line. An exact-location conditional exceedance is not established.
Yare near Reedham, eastern visit X14 EC25 25.28	M 2.27 to 7.00; P90 12.93 to 16.23. Exploratory reach transfer.	M 2.93 to 9.86; P90 14.71 to 19.80. Exploratory reach transfer.	Field lower limit 24.675 exceeds nominal actual-time P95 22.258, but the tidal-phase sensitivity maximum 32.303 accommodates the observation. The 1.76 km along-river transfer remains exploratory. Calendar-tail exceedance does not establish a tide-conditioned anomaly.
Yare near Reedham, western visit X15 EC25 25.19	M 2.16 to 6.31; P90 12.41 to 15.46. Exploratory reach transfer.	M 2.80 to 9.12; P90 14.17 to 18.93. Exploratory reach transfer.	Field lower limit 24.586 exceeds nominal actual-time P95 22.292, but the tidal-phase sensitivity maximum 30.862 accommodates it. The 1.32 km along-river transfer remains exploratory. Exact-location conditional rarity is unresolved.
Yare at New Cut junction V02, V08 EC25 27.93 to 32.54	M 2.39 to 7.74; P90 13.49 to 17.09. Exploratory junction model.	M 3.06 to 10.64; P90 15.26 to 20.76. Exploratory junction model.	Both visits exceed model drought-calendar P90s. V02 lower limit 27.331 exceeds nominal actual-time P95 25.642 but is accommodated by phase sensitivity 33.932. V08 central 32.538 is below nominal 33.843 and sensitivity 37.798. Junction exchange and the approximately 2.2 km transfer remain unresolved.
Lower Yare near Berney Arms V03 SP equiv. 32.06	AN-YAR2625 station model: M 20.02; P90 31.15. Reported ppt scale.	Station model: M 22.59; P90 33.47. Reported ppt scale.	Field SP equivalent 32.06 is below the model drought P90 33.47, although above sparse empirical drought percentiles. The station is 0.41 km away in straight line. Cross-method comparison and spatial transfer limit any exact-time local probability.
Waveney at Burgh Castle V04 SP equiv. 30.79	AN-WAV179 station model: M 18.92; P90 30.09. Reported ppt scale.	Station model: M 20.26; P90 31.20. Reported ppt scale.	Field SP equivalent 30.79 is below the model drought P90 31.20. It is high against the empirical summer distribution, but that is not the same as a conditional exceedance. Station separation is 0.30 km in straight line; exact-time local probability remains unresolved.
Lower Waveney near its mouth V05 SP equiv. 31.01	AN-WAV179 station model: M 18.92; P90 30.09. Reported ppt scale.	Station model: M 20.26; P90 31.20. Reported ppt scale.	Field SP equivalent 31.01 remains below model drought P90 31.20. The station is 1.14 km away in straight line. Its upper-estuary station distribution is context rather than a validated exact-coordinate, exact-time distribution.

Continued on the following page

Table 11 continued

Location and field observations	Q1: Normal conditions	Q2: Drought conditions	Q3: Comparison and limits
Lower Yare west of Berney Arms V06 SP equiv. 36.77	AN-YAR2625 station model: M 20.02; P90 31.15. Reported ppt scale.	Station model: M 22.59; P90 33.47. Reported ppt scale.	Field SP equivalent 36.77, with lower instrument limit 36.20, exceeds station-model drought P90 33.47. This supports an unusually high comparison value but does not establish an exact-location conditional tail probability. Salinity reconstruction and the station-to-visit transfer remain material.
Yare at Seven Mile Reach V07 SP equiv. 29.29	AN-YAR2625 station model: M 20.02; P90 31.15. Reported ppt scale.	Station model: M 22.59; P90 33.47. Reported ppt scale.	Field SP equivalent 29.29 is below the downstream station-model drought P90 33.47. The inland visit demonstrates polyhaline surface-water equivalents. A downstream comparator cannot establish its precise local rarity.
Reedham Ferry Reach V09 EC25 32.20	M 1.82 to 4.21; P90 10.71 to 13.25. Qualified coordinate model.	M 2.42 to 6.85; P90 12.34 to 16.51. Historical summer drought calendar.	Field lower limit 31.601 exceeds nominal actual-time P95 27.673 and the summer sensitivity maximum 29.734. A broader maximum-historical-error stress of 65.127 accommodates it. The result supports a conditional departure within the specified summer model family, not a universal physical upper limit.
Lower River Chet V15 EC25 10.37	Yare / Chet Mouth proxy: M 1.67 to 3.47; P90 8.28 to 12.43.	Mouth proxy: M 2.22 to 6.05; P90 10.36 to 15.01.	Field 10.370 establishes brackish surface water near the tributary mouth. The Yare confluence distribution has not been validated as a local Chet distribution. A local drought exceedance is not established.
Chet at Church Farm V16 EC25 11.33	Other-season local observations provide context; no defensible summer distribution.	No reliable local summer drought-tail estimate.	Field 11.330 is high relative to the available other-season context. Seasonally mismatched observations do not establish a local summer drought anomaly.
Chet near Loddon V17 EC25 5.61	Legacy marina proxy: M 0.971 to 0.983; P90 1.043 to 1.044.	Legacy marina proxy: M 0.994 to 1.008; P90 1.063 to 1.070.	Field 5.610 is far above the legacy comparator, including instrument lower limit 5.400. The comparator's marina setting and spatial transfer have not been validated for the sampled river coordinate. The large contextual departure is therefore qualified, not an exact-location drought-tail result.
Yare above Cantley V18 EC25 3.95	M 0.94 to 1.00; P90 1.39 to 2.15. Spatial mixture scenario.	M 0.99 to 1.02; P90 1.42 to 1.99. Spatial mixture scenario.	Field 3.950 exceeds the drought-calendar P90 range and narrower distance-mixture scenarios. Across retained endpoint and residual-transfer scenarios, actual-time P95 reaches 9.756 and summer sensitivity reaches 12.527. These contain the field value, so the anomaly is not robust to spatial transfer.
Fleet Dyke V19 EC25 1.479	No defensible local summer distribution.	No defensible local drought distribution.	Conductivity 1.479 is established for this surface sample. Local historical rarity and marine-ion attribution are not identified by the available evidence.
Coordinate 52.57848, 1.43802 V20 EC25 1.364	No geographic comparator assigned.	No geographic drought comparator assigned.	Conductivity 1.364 at 15:45 on 20 August is retained. The coordinate has not been assigned to a defensible waterbody or historical comparison. No geographic anomaly inference is made.

Continued on the following page

Table 11 continued

Location and field observations	Q1: Normal conditions	Q2: Drought conditions	Q3: Comparison and limits
Yare at Coldham Hall V21 EC25 1.316	M 0.854 to 0.858; P90 0.950 to 1.007. Qualified coordinate model.	M 0.919 to 0.928; P90 1.004 to 1.060. Summer drought calendar.	Field 1.316, lower limit 1.295, exceeds nominal actual-time P95 1.110 and summer sensitivity 1.261. Broader all-month phase/year sensitivity reaches 1.31644 and accommodates it. This is a qualified summer conductivity departure; freshwater-ion composition prevents a strong marine-salinity conclusion.
Yare at Bramerton V22 EC25 1.208	M 0.867 to 0.879; P90 0.991 to 1.170. Qualified coordinate model.	M 0.931 to 0.942; P90 1.053 to 1.228. Summer drought calendar.	Field 1.208 lies within the drought-calendar tail range, nominal actual-time P95 1.328 and summer sensitivity 2.167. No robust exceedance is identified.

I Additional evidence and its decision value

The companion `additional_data_requirements.csv` specifies 14 evidence requirements, including variables, periods, cadence, geographic and depth requirements, possible custodians, proposed operations and the conclusions they would improve. Availability is not assumed for unpublished material. The following priorities explain how additional evidence would change the central answer.

1. **Independent severe summer drought episodes.** Seek time-stamped salinity or reference-temperature conductivity, depth, local level and discharge from EA water-quality and hydrometry archives or relevant retained BFI inputs. Withhold entire drought episodes during model fitting and residual calibration. This would evaluate actual severe-drought upper-tail coverage at Chet Mouth and Reedham rather than borrowing errors from less severe conditions.

2. **Paired local spatial observations.** Seek synchronous measurements at boat and comparator positions, particularly the approximately 352 m Reedham and 329 m Coldham transfers and longer lower-Yare separations. Estimate within-reach differences against flow and tide, then withhold paired dates. This would test whether assumed smooth spatial transfer is valid near moving fronts.

3. **Oulton exchange and salinity history.** Seek archived Broad and Dyke salinity, water levels, lock or gate operations and relevant inflow information from EA, the Broads Authority or operators. Fit and validate a local exchange-aware expectation. This could distinguish an archive exceedance from a rare value under comparable drought and management conditions.

4. **Measurement reference and ionic composition.** Recover calibration and reference-setting records, or archived independent measurements of conductivity, chloride and major ions. Check the seawater-equivalent conversion and systematic bias. This is especially useful for the small Chet Mouth stress margin and low-conductivity inland observations; precise dilution volumes alone cannot resolve ionic composition.

5. **Antecedent forcing.** Seek final quality-controlled flow and sea-level records, plus catchment rainfall where available. Replace provisional or missing inputs, assess runoff lags and rerun the same frozen model family. This would narrow flow-state and coastal-gap sensitivities without conditioning on the field salinity response.

6. **Exposure and consequence records.** Seek continuous salinity, temperature and oxygen alongside fish, invertebrate and vegetation surveys, abstraction logs, crop and soil information. Estimate duration and recurrence at habitats or intakes, then test biological or agricultural outcomes. This would move the implications discussion from plausible mechanisms to local impact evidence.

No further targeted observations are presumed. With existing data, the paper reports the quantitative results above and preserves the uncertainty that these evidence requirements identify.

J Reproducibility and integrity review

The full archive contains the original workbook, frozen inputs, tables, renderers for 12 figures, the TikZ diagram, LaTeX and BibTeX sources and execution guides. The field rebuild reconciles all quantitative cells of the 36 observations against the workbook and verifies the 30 main inputs. The workbook SHA-256 identifier is `c5161485a9dc66361583b7e8fecff0ae9a2a6541f530abe7c2934801cc696781`. The unquantified V01 visit remains in the workbook but is not an analytical observation. Stable identifiers preserve provenance; no quantified sample is omitted.

The model supplement numerically refits the 64 field-comparable lower-Yare specifications in each of two coastal-input cohorts, giving 128 fits, all excluding 2026 responses. It regenerates whole-year and whole-station/year held-out predictions, the six reported primary nested-validation results, 5,632 field predictions and 192 historical-calendar quantile rows. The largest calendar discrepancy from the archived calculations is below 10^{-12} in the reported conductivity scale. It also refits 16 response-memory variants, checks 32 validation schemes and reproduces 704 dynamic field predictions. The complete declared X01 year-omission, coastal-error and joint-error protocols and the two-target Reedham/Chet protocol are rerun. A further 2,112 predictions reproduce six missing-flow scenarios, including the broader alternative that contains the Chet observation. These are internal numerical reproductions of the same methods, not independent scientific validation.

The reproduction boundary is explicit. Historical features, drought labels, paired calendar hours and forcing-error trajectories are frozen inputs. This is not a newly executed provider-to-result reconstruction of raw quality control, coastal gap filling, flow classification or every upper-Yare, Loddon and direct-estuary model. Original programs and archive/member hashes are supplied, but recovery is distinguished from execution. Retained outputs remain labelled. No public accession has been assigned.

The public supplement omits detailed NRFA-derived flow inputs under provider terms. It supplies the exclusion list, removed columns, original hashes and access/preparation instructions, while retaining code, coefficients, results and eligible chemistry and coastal data. The numerical reproductions above used the full working archive. Complete public model refits require separately obtained NRFA inputs and upstream preparation; the supplement is not self-contained for offline refitting.

The 216-scenario density calculation reproduces the original volume-weighted values, changes no class at the working reference and reports component mass-balance residuals. Instrument endpoints remain distinct from systematic sensitivities. Authored explanations for all 24 location groups are regenerated from a reviewed text table rather than presented as automatic statistical conclusions.

Internal checks covered completeness, original and derived quantities, precise preparation, surface sampling, temperature references, held-out populations and extrapolation. They separated empirical quantiles from error stresses, spatial spans from continuous plumes and climate implications from measured damage or attribution. Agreement supplies no new drought evidence. These AI-assisted checks are not independent human peer review.